HHS Public Access

Author manuscript

*Biol Psychiatry*. Author manuscript; available in PMC 2024 June 01.

Published in final edited form as:

*Biol Psychiatry*. 2023 June 01; 93(11): 976–988. doi:10.1016/j.biopsych.2022.12.008.

# Spinophilin limits metabotropic glutamate receptor 5 scaffolding to the postsynaptic density and cell type-specifically mediates excessive grooming

**Cameron W. Morris**[1], **Darryl S. Watkins**[1], **Nikhil R. Shah**[1,2], **Taylor Pennington**[3], **Basant Hens**[4], **Guihong Qi**[5,7], **Emma H. Doud**[5,7,9], **Amber L. Mosley**[5,7,8,9], **Brady K. Atwood**[3,4], **Anthony J. Baucum II**[3,4,6,*]

[1]Medical Neurosciences Graduate Program, Indiana University School of Medicine

[2]Medical Scientists Training Program, Indiana University School of Medicine

[3]Stark Neurosciences Research Institute (SNRI), Indiana University School of Medicine

[4]Department of Pharmacology and Toxicology, Indiana University School of Medicine

[5]Department of Biochemistry and Molecular Biology, Indiana University School of Medicine,

[6]Department of Biology, Indiana University-Purdue University Indianapolis

[7]Center for Proteome Analysis, Indiana University School of Medicine

[8]Center for Computational Biology and Bioinformatics, Indiana University School of Medicine

[9]Melvin and Bren Simon Comprehensive Cancer Center, Indiana University School of Medicine

## Abstract

**Background.—**Grooming dysfunction is a hallmark of the obsessive-compulsive spectrum disorder, trichotillomania. Numerous preclinical studies have utilized SAPAP3 deficient mice for understanding the neurobiology of repetitive grooming, suggesting excessive grooming is caused by increased metabotropic glutamate receptor 5 (mGluR5) activity in striatal direct- and indirect pathway medium spiny neurons (dMSNs and iMSNs, respectively). However, MSN subtype-specific signaling mechanisms that mediate mGluR5-dependent adaptations underlying excessive grooming are not fully understood. Here, we investigate the MSN subtype-specific roles of the striatal signaling hub protein, spinophilin, in mediating repetitive motor dysfunction associated with mGluR5 function.

**Methods.—**Quantitative proteomics and immunoblotting were utilized to identify how spinophilin impacts mGluR5 phosphorylation and protein interaction changes. Plasticity and

*To whom correspondence should be sent: Anthony J. Baucum II, Ph.D. Department of Pharmacology and Toxicology, 635 Barnhill Dr. Indianapolis, IN 46202. ajbaucum@iupui.edu. 317-274-0540.



Competing Interests

The authors report no biomedical financial interests or potential conflicts of interest.

repetitive motor dysfunction associated with mGluR5 action was measured using our novel conditional spinophilin mouse model that had spinophilin knocked out from striatal dMSNs or/and iMSNs.

**Results.—**Loss of spinophilin only in iMSNs decreased performance of a novel motor repertoire, but loss of spinophilin in either MSN subtype abrogated striatal plasticity associated with mGluR5 function and prevented excessive grooming caused by SAPAP3 knockout mice or treatment with the mGluR5-specific positive allosteric modulator (VU0360172) without impacting locomotion-relevant behavior. Biochemically, we determined the spinophilin-mGluR5 interaction correlates with grooming behavior and loss of spinophilin shifts mGluR5 interactions from lipid-raft associated proteins toward postsynaptic density (PSD) proteins implicated in psychiatric disorders.

**Conclusions.—**These results identify spinophilin as a novel striatal signaling hub molecule in MSNs that cell subtype-specifically mediates behavioral, functional, and molecular adaptations associated with repetitive motor dysfunction in psychiatric disorders.

### Keywords

signaling; phosphatase targeting proteins; postsynaptic density; plasticity; striatum; trichotillomania

## Introduction

The sensorimotor striatum, a major basal ganglia input nucleus, integrates excitatory and modulatory inputs from diverse cortical and subcortical structures to promote the learning and execution of complex tasks (1, 2). Perturbations within the sensorimotor striatum, or the rodent dorsolateral striatum (DLS), are associated with repetitive motor dysfunction in numerous psychiatric disorders, including obsessive-compulsive spectrum disorders (OCSDs) (3–12). Cell type-specific adaptations in striatal direct- and indirect-pathway medium spiny neurons (dMSNs and iMSNs, respectively) within the DLS underlie repetitive and habitual actions (13–19). Functionally, dMSNs, which express D1-type dopamine receptors (D1Rs), promote action execution by increasing thalamic neuronal firing rates, which in turn increase glutamatergic tone in the cortex; whereas, iMSNs, which express D2-type dopamine receptors (D2Rs), inhibit or temper competing motor programs by promoting the inhibition of thalamic output to the cortex, thus decreasing glutamatergic drive (20–25). Despite bidirectional actions on basal ganglia output, dMSNs and iMSNs work in concert to integrate glutamatergic and dopaminergic signaling to promote complex motor programs, and signaling molecule perturbations within MSNs can increase the propensity to repetitively execute previously learned motor sequences, a core motor phenotype associated with OCSDs (1, 26–36).

Dysfunction in metabotropic glutamate receptor 5 (mGluR5) signaling and/or its interaction with postsynaptic density (PSD) scaffolding proteins is associated with repetitive motor dysfunction in numerous preclinical models for understanding psychiatric disorders (19, 37–42). Of these, mutations in the striatal-enriched mGluR5 scaffold protein, disks large-associated protein 3 (SAPAP3), are associated with repetitive grooming and washing symptoms in OCSDs (43–45). Genetic deletion of SAPAP3 in mice results in striatal circuit

abnormalities and increased mGluR5 function that promotes excessive grooming (13, 46–52), a complex sequential motor program that becomes excessively initiated and sustained despite negative consequences (53).

Reversible phosphorylation of mGluR5's intracellular C-terminal domain is a negative feedback mechanism that promotes receptor desensitization (54–56). Protein phosphatases, such as protein phosphatase 1 (PP1), can reverse this endocytic feedback mechanism to stabilize mGluR5 on the membrane surface (57). Promiscuous phosphatases require targeting proteins to shuttle them into contact with their targets (58). However, the role(s) phosphatase targeting proteins play in promoting increased mGluR5 function to mediate repetitive motor dysfunction are unknown.

Spinophilin is a striatal PSD signaling hub molecule that targets PP1 to diverse substrates (59–64). Spinophilin promotes plasticity and motor behaviors associated with DLS function, stabilizes mGluR5 expression in the neuronal membrane, and prevents G-protein coupled receptor (GPCR) desensitization (65–74). Recently, we determined that spinophilin interacts with SAPAP3 in mouse striatum, and overexpression of a glutamate binding deficient mGluR5 construct increased the spinophilin-SAPAP3 protein interaction (67). However, how endogenous spinophilin mediates striatal plasticity and SAPAP3- and mGluR5-dependent repetitive motor output is unknown. Here, using a novel conditional spinophilin knockout mouse line, combined with behavioral, functional, biochemical, and proteomic approaches, we implicate spinophilin as a hub striatal signaling molecule that mediates MSN subtype-specific adaptations underlying repetitive motor output associated with increased mGluR5 function.

## Materials and Methods

Refer to supplement for complete report.

### Animals

All animal procedures were performed on 7-16 week-old male and female mice between 8AM and 5PM in accordance with the School of Science, School of Medicine, and Institutional Animal Care and Use Committees at IUPUI (Protocol #s SC270R, SC310R, 21090).

### Animal Behavior

Rotarod was performed as previously described (66). Locomotion and grooming measures were performed in Noldus Phenotyper Cages.

### Electrophysiology

Electrophysiology experiments were performed as previously described (75, 76).

### Tissue Homogenization, Immunoprecipitations, and Immunoblotting

Homogenization, immunoprecipitation, and immunoblotting were performed like previously described (64, 67, 77, 78).

### Proteomics

Proteomics analysis was performed at the Center for Proteome Analysis at IUSM similar to previously published protocols (77, 79).

### RNAScope and Imaging

RNAScope was performed per manufacturer's (Advanced Cell Diagnostics, Newark, CA) recommendations.

### Statistics

All statistical analyses are described fully in supplement and all analyses shown in Table S6. Male and female mice were used for all behavior experiments and while sex was not considered as a biological variable in the present study, data are separated by sex in supplemental figures.

## Results

### Spinophilin has MSN-specific roles in mediating motor function and striatal plasticity.

Spinophilin is expressed in diverse brain regions and cell types (59, 80–82). To directly probe spinophilin's MSN-specific functions we created and validated a conditional spinophilin line (Spino$^{Fl/Fl}$), which is fully described in the supplemental results and discussion sections. Briefly, we biochemically validated Spino$^{Fl/Fl}$ mice by demonstrating a robust Cre recombinase-dependent depletion of spinophilin protein levels (Figure S1). We next bred Spino$^{Fl/Fl}$ mice with Drd1- or Adora2a-Cre lines to deplete spinophilin from dMSNs (Spino$^{\Delta dMSN}$) or iMSNs (Spino$^{\Delta iMSN}$), respectively. Using RNAScope we validated the penetrance of D1- and A2A-Cre (~80-85%) and confirmed cell-autonomous depletion of spinophilin mRNA in Spino$^{\Delta dMSN}$ and Spino$^{\Delta iMSN}$ mice (Figures S2–7). Spinophilin protein expression was significantly reduced (~25%) in spino$^{\Delta dMSN}$ and spino$^{\Delta iMSN}$ mice; however, PP1 protein levels were unaffected (Figure 1A–E). Consistent with these data, spinophilin protein levels were reduced by ~40% in Spino$^{Fl/Fl}$ mice expressing both D1- and A2A-Cre (Figure S8). Taken together, these data demonstrate spinophilin is depleted cell autonomously but a proportion of spinophilin is expressed in other cell types within the striatum (e.g. interneurons, terminals, and/or glia).

We next characterized motor function in Spino$^{\Delta dMSN}$ and Spino$^{\Delta iMSN}$ mice by challenging these genotypes with an accelerating rotarod task and amphetamine-induced locomotor sensitization (Figure 1F), behaviors that whole-body spinophilin knockout (Spino$^{-/-}$) decreases (66–68). Spino$^{\Delta iMSN}$, but not Spino$^{\Delta dMSN}$, mice had decreased rotarod performance in the later stages of this motor task (Figure 1G, S9). However, both Spino$^{\Delta dMSN}$ and Spino$^{\Delta iMSN}$ mice displayed acute hyperlocomotion and locomotor sensitization to treatment with repeated doses of amphetamine (Figure 1H).

To measure spinophilin's MSN subtype-specific roles in regulating DLS network excitability and long-term plasticity, we recorded field population spike amplitude responses to stimulation and long-term synaptic depression (LTD), a form of striatal plasticity that requires increased mGluR5 and D2-dopamine receptor ($D_2R$) function (83, 84). Specifically,

we recorded population spike amplitudes evoked from increasing electrical stimulation intensities (input/output) or high-frequency stimulations that induce LTD (HFS-LTD) in coronal sections from control, Spino$^{\Delta dMSN}$, and Spino$^{\Delta iMSN}$ mice. We detected a spino genotype X intensity interaction suggesting Spino$^{\Delta dMSN}$ increases DLS network responses; however, we did not detect any post-hoc genotype differences within intensity groups (Figure 1I). Both Spino$^{\Delta dMSN}$ and Spino$^{\Delta iMSN}$ mice had significantly decreased HFS-LTD compared to Spino$^{Fl/Fl}$ control. Unlike control, the population spike amplitude did not decrease in Spino$^{\Delta dMSN}$ or Spino$^{\Delta iMSN}$ mice following either single or multiple bouts of high-frequency stimulation (Figure 1J–N).

### Spinophilin dMSN- and iMSN-KO decreases excessive grooming in SAPAP3 KO mice.

Excessive grooming and hypolocomotion in SAPAP3 KO mice are associated with increased mGluR5 signaling and plasticity in the DLS (13, 46). Given that spinophilin interacts with SAPAP3 in mouse striatum, mGluR5 expression increases the spinophilin-SAPAP3 protein interaction, and MSN subtype-specific spinophilin knockout decreases DLS plasticity, we hypothesized that MSN subtype-specific loss of spinophilin would decrease excessive grooming in SAPAP3 KO mice.

We first measured basal grooming and locomotion levels from Spino$^{-/-}$ mice in Noldus Phenotyper cages for 30-minutes using a validated AI approach (Figures 2A, S10). Loss of spinophilin decreased the percentage of time grooming over the entire session (percent grooming) (Figure 2B). The percentage of time spent grooming is determined, at least in part, by the number of grooming bouts (grooming frequency) and the mean duration of an individual grooming bout (mean bout duration); however, we found no difference in grooming frequency or mean grooming bout duration in Spino$^{-/-}$ mice (Figure 2C–D). Alternatively, Spino$^{-/-}$ mice had significantly increased locomotion relative to controls (Spino$^{+/+}$) (Figure 2E).

We next utilized our conditional spinophilin line to generate double knockout mice (SAPAP3 WT and KO/spinophilin MSN subtype-specific KO) to determine if spinophilin in specific MSN subtypes impacts basal and/or excessive grooming. At 8-weeks of age, grooming and locomotion was measured for 1-hour (Figure 2F). Constitutive knockout of SAPAP3 significantly increased percent grooming in spinophilin control and Spino$^{\Delta dMSN}$ mice compared to their genotype controls, whereas the increased percent grooming was abrogated in Spino$^{\Delta iMSN}$ mice compared to their genotype controls. Although percent grooming in SAPAP3 WT controls was not different than SAPAP3 WT/Spino$^{\Delta dMSN}$ and SAPAP3 WT/Spino$^{\Delta iMSN}$ mice, percent grooming was significantly decreased in both SAPAP3 KO/Spino$^{\Delta dMSN}$ and SAPAP3 KO/Spino$^{\Delta iMSN}$ mice compared to SAPAP3 KO/spinophilin control mice (Figure 2G). This was a spinophilin-specific effect as D1- or A2A-Cre expression alone didn't decrease excessive grooming in SAPAP3 KO mice (Figure S11).

We detected SAPAP3 genotype and spinophilin genotype effects on both grooming frequency and mean bout duration, such that *grooming frequency* was significantly reduced in SAPAP3 KO/Spino$^{\Delta iMSN}$ and *mean bout duration* was significantly reduced in SAPAP3

WT/Spino$^{\Delta dMSN}$ compared to SAPAP3 WT mice, and in both SAPAP3 KO/Spino$^{\Delta dMSN}$ and SAPAP3 KO/Spino$^{\Delta iMSN}$ compared to SAPAP3 KO/spinophilin WT mice (Figure H–I).

In addition to grooming dysfunction, we detected SAPAP3 genotype effects causing hypolocomotion in control, Spino$^{\Delta dMSN}$, and Spino$^{\Delta iMSN}$ mice. SAPAP3 KO/Spino$^{\Delta iMSN}$ mice had small, but significantly increased locomotion compared to SAPAP3 KO control mice (Figure 2J). Given that grooming and locomotion are competing behaviors in the OF, we correlated distance traveled and grooming duration for each genotype, but we only detected a significant negative correlation in SAPAP3 WT and SAPAP3 KO/Spino$^{\Delta iMSN}$ (Figure 2K–L). Grooming and locomotion data were also analyzed in 30-minute bins to confirm genotype differences are consistent between the first and second halves of recording (Figure S12).

## The interaction of spinophilin with mGluR5 is increased in SAPAP3 KO striatum and correlates with grooming duration.

Given that increased striatal mGluR5 signaling is associated with grooming dysfunction in SAPAP3 KO mice we measured spinophilin's interaction with mGluR5 in SAPAP3 KO striatum. In addition, we measured spinophilin's interaction with the $D_2R$ (85)—another striatal GPCR known to decrease rodent grooming (86). We harvested striata from 4-6 month-old SAPAP3 WT and KO mice following measurement of grooming behavior and measured the expression and interaction of spinophilin with these GPCRs as well as PP1$\gamma$1 (Figures 3A–B, S13). Quantitative immunoblot analysis of striatal input samples determined that SAPAP3 KO did not affect spinophilin, mGluR5, or $D_2R$ expression; however, PP1$\gamma$1 expression was significantly increased in SAPAP3 KO mice (Figure 3C–F). Although we found no change in spinophilin's interaction with PP1$\gamma$1, there was significantly more mGluR5 and $D_2R$ in spinophilin IPs from SAPAP3 KO striatum (Figure 3G–I). We detected minimal PP1$\gamma$1, mGluR5, or $D_2R$ co-IP in spinophilin IPs from Spino$^{-/-}$ striatal tissue (Figure 3A, lane 3), indicating co-IPs are specific. Moreover, we found a significant Pearson's correlation between percent grooming and the $\log_2$ fold-change in the spinophilin-mGluR5 or spinophilin-$D_2R$ interaction (Figure 3J–K) as well as a significant correlation between the spinophilin-mGluR5 and spinophilin-$D_2R$ interaction (Figure 3L).

## Loss of spinophilin modulates mGluR5 phosphorylation.

To probe consequences of loss of spinophilin on mGluR5, we measured mGluR5 phosphorylation in Spino$^{+/+}$ and Spino$^{-/-}$ striatum. First, we performed striatal mGluR5 IPs from one Spino$^{+/+}$ and Spino$^{-/-}$ mouse and excised the mGluR5 band on a Coomassie gel for a targeted GelC-MS run to validate that we can ratiometrically quantify phosphorylation sites on mGluR5 (Figures S14–17). Preliminarily, we determined that loss of spinophilin increased mGluR5 phosphorylation at Ser860 and Ser870 (Table S1). To follow up on these preliminary results, we pooled sequential mGluR5 IPs from Spino$^{+/+}$ and Spino$^{-/-}$ striatal lysates (N=3 per genotype). These sequential IPs immunodepleted mGluR5 by ~80%, and we found no genotype difference in immunodepletion or mGluR5 expression (Figures 4A–C, S18). mGluR5 complexes were submitted for protein identification and ratiometric quantification using tandem mass tag-liquid chromatography/mass spectrometry (TMT-LC/MS). Given the inherent variability of IPs coupled with TMT-LC/MS (87), we

utilized a $Log_2$ Abundance Ratio (KO/WT) < −0.2 or > 0.2 combined with one-tailed t-tests ($\alpha$<0.10) to identify decreased or increased phosphopeptides, respectively. While we did not detect Ser870 phosphorylation in our TMT proteomics analysis, potentially due to signal suppression of this phosphopeptide as it is not from an excised band sample, we did observe that loss of spinophilin increased the abundance of mGluR5 Ser860 and Ser1016 phosphorylation, as well as SHANK3 Ser781 and SAPAP2 Ser983, proteins with strong genetic associations with autism spectrum disorders (ASDs) and OCSDs (88–94) (Figure 4D).

## Loss of spinophilin shifts mGluR5 interactions from lipid raft assemblies toward PSD scaffolding proteins implicated in psychiatric disorders.

We next analyzed protein abundance of mGluR5 co-IPs in the TMT-LC/MS dataset, which can give insight into consequences of loss of spinophilin on mGluR5 function. We identified 92 downregulated ($log_2$-fold change < −0.2) and 426 upregulated ($log_2$-fold change > 0.2) mGluR5 co-IPs isolated from $Spino^{-/-}$ striatum that resulted in expansive protein-protein interaction (PPI) networks (Figures S19–20). We filtered this list of interactors for significantly decreased/increased proteins (p<0.10 from one-tailed t-tests) that matched at least 6 unique peptides. We identified 27 decreased and 22 increased high-confidence mGluR5 interactors in $Spin^{-/-}$ striatum (orange and green points in Figure 4E, respectively). We utilized STRING-DB to generate decreased and increased PPI networks that were used for functional enrichment analysis (Figure 4F–I, Table S3–4). We determined that spinophilin knockout decreased mGluR5 interactions with glycosylphosphatidylinositol (GPI)-anchored proteins, a class of proteins localized to specialized microdomains in the plasma membrane known as lipid rafts (95) including contactin-1, Thy1, and flotillin-1, and increased mGluR5 interactions with PSD scaffolding proteins, including SAPAP3, SHANK3, and Homer1. Interestingly, shifting mGluR5 interactions toward PSD proteins in $Spino^{-/-}$ striatum was associated with multiple Biological Process GO terms, one of which was “regulation of grooming behavior”. We validated increased and decreased mGluR5 interactions by normalizing data from two TMT-LC/MS runs (Figure S21A–F, Table S5). Moreover, immunoblotting inputs and mGluR5 IPs (Figure 4J, S21I) from $Spino^{-/-}$ striatum confirmed that loss of spinophilin decreased the expression of the lipid raft marker, flotillin-1, and increased the mGluR5 interaction with Homer 1b/c, without impacting Homer1b/c expression, similar to TMT-LC/MS studies (Figure 4K–M, S21G–H).

## Spinophilin MSN-specifically Decreases Grooming Caused by the mGluR5 Positive Allosteric Modulator (PAM), VU0360172 (VU`172).

To directly determine if spinophilin mediates mGluR5-dependent excessive grooming, we pharmacologically increased grooming behavior by treating mice with the mGluR5 PAM, VU’172, that selectively increases grooming in wild type, but not mGluR5-KO mice (13). Specifically, we measured grooming behavior in control, $Spino^{\Delta dMSN}$, $Spino^{\Delta iMSN}$, and $Spino^{-/-}$ mice for 30-minutes before and after an I.P. injection of vehicle or VU’172 (20 mg/kg) (Figure 5A). While baseline percent grooming and distance traveled were increased in $Spin^{-/-}$ compared to control, $Spino^{\Delta dMSN}$, and $Spino^{\Delta iMSN}$ mice, we did not detect any pre-existing treatment group effects (Figure S22). Vehicle treatment increased grooming (a grooming phenotype that is also decreased in mGluR5-KO mice); however, grooming

was further increased by VU'172 treatment in Spino$^{Fl/+ \text{ or } Fl/Fl}$ and Spino$^{+/+}$/D1- or A2A-Cre control mice (Figure 5B, S23). Interestingly, we also observed an increase grooming response to VU'172 in Spino$^{-/-}$ mice. Furthermore, we detected significant treatment X spinophilin genotype interaction on percent grooming, such that we did not detect a VU'172 treatment effect on percent grooming in Spino$^{\Delta dMSN}$ or Spino$^{\Delta iMSN}$ mice, and percent grooming in VU'172-treated Spino$^{\Delta dMSN}$ and Spino$^{\Delta iMSN}$ mice was not significantly different from vehicle-treated control mice (Figure 5B). Post-injection percent grooming data were also analyzed in 5-minute bins to confirm genotype effects were consistent across the 30-minute recording (Figure S24). Collectively, these data suggest MSN subtype-specific spinophilin knockout, but not global knockout, abrogates VU'172-induced grooming. Although we detected a significant treatment effect on grooming frequency, we found no genotype or genotype X treatment interaction (Figure 5C). Furthermore, neither VU'172 (20 mg/kg) nor spinophilin genotype affected mean grooming bout duration (Figure 5D).

To better understand why Spino$^{-/-}$ mice, but not Spino$^{\Delta dMSN}$ and Spino$^{\Delta iMSN}$ mice, respond to VU'172, we bred Spino$^{\Delta dMSN}$ and Spino$^{\Delta iMSN}$ mice to knockout spinophilin from both MSN subtypes (Spino$^{\Delta PanMSN}$) and treated this genotype with vehicle or VU'172 (20 mg/kg). Again, loss of spinophilin in both MSN subtypes did not prevent the VU'172 treatment effect on percent grooming or grooming frequency (Figure 5E–H, S25). Collectively, these data confirm that only MSN subtype-specific loss of spinophilin prevents VU'172 treatment effect, consistent with other reports suggesting an imbalance in MSN function may be associated with repetitive grooming behavior (13, 18, 96).

Finally, we performed a VU'172 dose response curve (DRC) in Spino$^{Fl/Fl}$ control mice using a dose range consistent with published studies using VU'172 in mice (97–99) to find percent grooming at low doses is driven by increased mean grooming bout duration, whereas, at high doses, percent grooming is driven by increased grooming frequency (Figure S26). To determine the directionality by which MSN subtype-specific spinophilin knockout shifts the VU'172 DRC we treated new cohorts of Spino$^{\Delta dMSN}$ and Spino$^{\Delta iMSN}$ with a low (1 mg/kg) or high (56 mg/kg) dose of VU'172 and combined these data with our existing 20 mg/kg data (Figure 5B–D) to create a 4-point DRC for percent grooming, grooming frequency, and mean grooming bout duration (Figure 5I–K). We determined that Spino$^{\Delta dMSN}$ decreased percent grooming compared to control. Although the two-way ANOVA did not detect spinophilin genotype effects or interactions on grooming frequency or mean grooming bout duration, we found a within-dose Spino$^{\Delta dMSN}$ genotype effect on mean bout duration at 1 mg/kg and a trend for decreased grooming frequency at 20 mg/kg (Figure S27), suggesting Spino$^{\Delta dMSN}$ may decrease percent grooming via dose-specific mechanisms.

Given that grooming and locomotion are competing behaviors in the OF, we also analyzed distance traveled in 20 mg/kg VU'172-treated animals. Although we detected a significant treatment, genotype, and interaction effect on locomotion in OF, post-hoc tests found no significant differences in Spino$^{\Delta dMSN}$ and Spino$^{\Delta iMSN}$ compared to control, but rather attributed ANOVA effects to increased locomotion in vehicle-treated Spino$^{-/-}$ mice (Figure S28). Furthermore, MSN subtype-specific loss of spinophilin did not disrupt the negative relationship between grooming duration and distance traveled.

## Discussion

Here, we report that decreased mGluR5-dependent repetitive grooming in Spino$^{\Delta dMSN}$ and Spino$^{\Delta iMSN}$ mice is associated with the reversal of numerous molecular and functional phenotypes associated with SAPAP3 deficient mice (Figure 6). Excessive grooming in SAPAP3 KO mice is associated with MSN subtype-specific adaptations that increase dMSN function relative to neighboring iMSNs in the DLS (13). Both striatal abnormalities —excessive grooming and increased dMSN function—are decreased by treatment with the mGluR5 negative allosteric modulator (NAM), MTEP (13). We determined that spinophilin's protein interaction with mGluR5 is increased in SAPAP3 KO mice, and that MSN subtype-specific spinophilin knockout also prevents increased grooming duration caused by the mGluR5-specific PAM, VU'172. Collectively, these data suggest that spinophilin expression in striatal MSNs mediates mGluR5-dependent excessive grooming.

Given that whole-body loss of spinophilin decreased basal grooming and MSN subtype-specific spinophilin knockout prevented excessive grooming in SAPAP3 KO mice and VU'172-treated mice (20 mg/kg), it was unexpected that whole-body loss of spinophilin failed to decrease VU'172 grooming. We further confirmed that this effect was not due to extra-striatal spinophilin functions by demonstrating a VU'172 treatment effect on grooming in Spino$^{\Delta PanMSN}$ mice. We further probed this surprising effect by comparing 4-point VU'172 dose response curve (DRC) from control, Spino$^{\Delta dMSN}$, and Spino$^{\Delta dMSN}$ mice. Surprisingly, we found unique DRCs across these genotypes, such that Spino$^{\Delta dMSN}$ significantly decreased the percent grooming DRC, whereas the Spino$^{\Delta iMSN}$ effect on percent grooming was specific to the 20 mg/kg dose. Therefore, while global loss of spinophilin may limit basal grooming by affecting non-MSN cell-types, MSN subtype-specific loss of spinophilin may limit mGluR5-dependent grooming by preventing a shift in the balance between iMSNs and dMSNs, an effect observed in multiple excessive grooming models (13, 18).

Increased grooming duration (percent grooming) is achieved, at least in part, by increased grooming bout initiation (grooming frequency) or by sustained grooming bouts (mean bout duration). Although Spino$^{-/-}$ mice did not impact grooming frequency or mean bout duration, Spino$^{\Delta dMSN}$ and Spino$^{\Delta iMSN}$ differentially impacted grooming microstructure. Increased dMSN function is essential for initiating and sustaining complex motor programs, including rodent self-grooming (16, 86, 100). Spino$^{\Delta dMSN}$ mice decreased mean bout duration both in SAPAP3 KO mice and mice treated with 1 mg/kg VU'172, suggesting spinophilin expression in dMSNs may sustain complex motor programs. In contrast, further suggesting .

Decreasing iMSN function with a $D_2R$ agonist decreases grooming initiation, duration, and sequence completion (86, 100). Interestingly, spinophilin's interaction with $D_2R$ was increased in SAPAP3 KO striatum and correlated with grooming behavior. Furthermore, Spino$^{\Delta iMSN}$ mice decreased grooming frequency and mean bout duration in SAPAP3 KO mice and blunted the performance of an accelerating rotarod task, another sequential motor behavior associated with $D_2R$ function (101), suggesting spinophilin expression in iMSNs may be critical for executing and completing complex sequential motor programs.

Recently, Tecuapetla and colleagues determined that optogenetic inhibition of striatal iMSNs in the dorsomedial striatum (DMS) decreased excessive grooming in SAPAP3 KO mice (96). While we have identified that MSN subtype-specific loss of spinophilin decreases excessive grooming, it is unclear if spinophilin functions in specific striatal subregions to mediate excessive grooming. Furthermore, while the D1- and A2A-Cre lines utilized herein are highly expressed within striatal dMSNs or iMSNs, it is possible that spinophilin mediates excessive grooming by functioning in cell types outside the striatum through residual extra-striatal Cre expression or in a non-cell-autonomous manner. However, both Spino$^{\Delta dMSN}$ and Spino$^{\Delta iMSN}$ mice had abrogated HFS-LTD in the DLS—plasticity that requires mGluR5 and $D_2$R function (83, 84). The role of decreased LTD limiting pathological grooming is consistent with studies showing that SAPAP3 KO mice undergo *increased* short-term plasticity due to increased mGluR5 function in the DLS (46). Furthermore, the increased DLS network responses in Spino$^{\Delta dMSN}$ mice is also an opposite phenotype of preclinical excessive grooming models (52, 102). Future studies will build upon the foundation laid herein to delineate spinophilin's cell-autonomous and non-autonomous functions in specific striatal subregions in mediating plasticity associated with repetitive motor dysfunction.

Spinophilin knockout-derived primary cortical neurons have increased mGluR5-dependent MAPK signaling and intracellular calcium mobilization ([$Ca^{2+}$]) that leads to increased mGluR5 endocytosis (69). Loss of spinophilin upregulated striatal mGluR5 phosphorylation at Ser860 (a predicted protein kinase A consensus site), Ser1016 (a published CaMKII site (103)), and Ser839 and Ser908 (protein kinase C sites (104, 105)). Although the function of mGluR5 Ser860 phosphorylation is unknown, phosphorylation of Ser1016, 839, and 908 promote increased MAPK signaling, $[Ca^{2+}]_i$ mobilization, and mGluR5 desensitization (54, 55, 103–105). Future studies will elucidate how phosphorylation of these mGluR5 sites govern its signaling, interactions, and localization within the postsynaptic membrane. Moreover, as PP1 catalytic subunits are highly promiscuous and spinophilin interacts with multiple proteins, the full panoply of spinophilin actions on mGluR5-dependent function are most likely not restricted to just mGluR5 phosphorylation and interactions, but also may impact actions downstream of mGluR5 activation.

Excessive grooming in both SAPAP3 KO and SHANK3 complete KO mice—preclinical models for understanding OCSDs and ASDs, respectively—is decreased by mGluR5 NAMs. Grooming dysfunction in both these preclinical models is associated with decreased mGluR5 scaffolding to PSD proteins (13, 19). Interestingly, loss of spinophilin increased mGluR5 interactions with PSD scaffolding proteins implicated in psychiatric disorders, including SAPAP3, SHANK3, and Homer 1b/c, and decreased mGluR5 interactions with lipid raft-associated membrane proteins, such as flotillin in the striatum. Not only is lipid raft dysfunction associated with psychiatric disorders like the ASD, fragile X syndrome (42, 106–108), mGluR5 can differentially signal depending on its interactions with lipid raft signaling complexes or PSD scaffolding proteins, such that increased mGluR5-Homer 1b/c interaction promotes MAPK signaling (109–111). Interestingly, increased ERK activity is associated with excessive grooming in SHANK3 complete KO mice, and spinophilin is suggested to occlude increases in MAPK signaling following repeated doses of psychostimulants (19, 68). Although basal grooming was decreased in Spino$^{-/-}$ mice, one

caveat of these proteomics data is that global loss of spinophilin did not affect VU'172-induced grooming. However, we posit that loss of spinophilin is inducing similar changes in mGluR5 interactions in dMSNs and iMSNs, but that spinophilin MSN subtype-specifically mediates excessive grooming by preventing the shift in the balance of activity between these two MSN populations in the context of mGluR5 treatment, an effect that may link to the bidirectional actions of these neuronal populations on motor output (112).

Although MSN subtype-specific spinophilin KO decreased two models of excessive grooming associated with increased mGluR5 function, neither Spino$^{\Delta dMSN}$ nor Spino$^{\Delta iMSN}$ affected basal, hypo-, or hyper-locomotion. Therefore, we hypothesize that MSN subtype-specific spinophilin knockout selectively disrupts complex sequential motor programs without impacting overall locomotor output. Due to this, we postulate that our novel MSN subtype-specific spinophilin knockout models are a valuable tool to elucidate unique cell autonomous and/or non-autonomous signaling pathways underlying the initiation, sustainment, and/or completion of sequential motor programs.

## Supplementary Material

Refer to Web version on PubMed Central for supplementary material.

## Acknowledgements

Mass spectrometry work performed herein was done by the Indiana University School of Medicine Center for Proteome Analysis. Acquisition of the IUSM Proteomics instrumentation used for this project was provided by the Indiana University Precision Health Initiative. The proteomics work was supported, in part, by the Indiana Clinical and Translational Sciences Institute funded, in part by Award Number UL1TR002529 from the National Institutes of Health, National Center for Advancing Translational Sciences, Clinical and Translational Sciences Award and the Cancer Center Support Grant for the IU Simon Comprehensive Cancer Center (Award Number P30CA082709) from the National Cancer Institute. We acknowledge and thank Wanda Filipiak & Galina Gavrilina for embryo injections for the initial generation of Spino$^{Fl/Fl}$ mice as well as the entire excellent Transgenic Animal Model Core (in particular, Anna LaForest, Elizabeth Hughes, Corey Ziebell, and Dr. Thomas Saunders) and the University of Michigan's Biomedical Research Core Facilities for their generation of these mice. Funding for the generation of these mice and completion of studies comes from an R21/R33 award from the National Institutes of Drug Abuse (R21/R33 DA041876 to AJB), Department of Biology/School of Science at IUPUI, Department of Pharmacology and Toxicology Startup Funds, Strategic Research Initiative Funds (Indiana University School of Medicine and Stark Neurosciences Research Institute). We thank Dr. Benjamin Liffner and Dr. Sabrina Absalon for training and troubleshooting on the confocal microscope. We acknowledge Emily Claeboe for lab support and appreciate the feedback from all members of the Baucum laboratory over the years on this project.

## Data Availability

Proteomics datasets from GelC-MS, TMT-LC/MS run 1, and TMT-LC/MS run 2 experiments were uploaded to ProteomeXchange (PXD034053 and 10.6019/PXD034053).

## References

1. Graybiel AM (2008): Habits, rituals, and the evaluative brain. Annu Rev Neurosci. 31:359–387. [PubMed: 18558860]
2. Jahanshahi M, Obeso I, Rothwell JC, Obeso JA (2015): A fronto–striato–subthalamic–pallidal network for goal-directed and habitual inhibition. Nature Reviews Neuroscience. 16:719. [PubMed: 26530468]

3. Abbott AE, Linke AC, Nair A, Jahedi A, Alba LA, Keown CL, et al. (2018): Repetitive behaviors in autism are linked to imbalance of corticostriatal connectivity: a functional connectivity MRI study. Soc Cogn Affect Neurosci. 13:32–42. [PubMed: 29177509]
4. Anticevic A, Hu S, Zhang S, Savic A, Billingslea E, Wasylink S, et al. (2014): Global resting-state functional magnetic resonance imaging analysis identifies frontal cortex, striatal, and cerebellar dysconnectivity in obsessive-compulsive disorder. Biol Psychiatry. 75:595–605. [PubMed: 24314349]
5. Beucke JC, Sepulcre J, Talukdar T, Linnman C, Zschenderlein K, Endrass T, et al. (2013): Abnormally high degree connectivity of the orbitofrontal cortex in obsessive-compulsive disorder. JAMA Psychiatry. 70:619–629. [PubMed: 23740050]
6. O'Sullivan RL, Rauch SL, Breiter HC, Grachev ID, Baer L, Kennedy DN, et al. (1997): Reduced basal ganglia volumes in trichotillomania measured via morphometric magnetic resonance imaging. Biological Psychiatry. 42:39–45. [PubMed: 9193740]
7. Sakai Y, Narumoto J, Nishida S, Nakamae T, Yamada K, Nishimura T, et al. (2011): Corticostriatal functional connectivity in non-medicated patients with obsessive-compulsive disorder. Eur Psychiatry. 26:463–469. [PubMed: 21067900]
8. Atmaca M, Yildirim H, Ozdemir H, Tezcan E, Poyraz AK (2007): Volumetric MRI study of key brain regions implicated in obsessive-compulsive disorder. Prog Neuropsychopharmacol Biol Psychiatry. 31:46–52. [PubMed: 16859819]
9. Pujol J, Soriano-Mas C, Alonso P, Cardoner N, Menchon JM, Deus J, et al. (2004): Mapping structural brain alterations in obsessive-compulsive disorder. Arch Gen Psychiatry. 61:720–730. [PubMed: 15237084]
10. Harrison BJ, Pujol J, Cardoner N, Deus J, Alonso P, Lopez-Sola M, et al. (2013): Brain corticostriatal systems and the major clinical symptom dimensions of obsessive-compulsive disorder. Biol Psychiatry. 73:321–328. [PubMed: 23200527]
11. Di Martino A, Kelly C, Grzadzinski R, Zuo X-N, Mennes M, Mairena MA, et al. (2011): Aberrant striatal functional connectivity in children with autism. Biological psychiatry. 69:847–856. [PubMed: 21195388]
12. Grossberg S, Kishnan D (2018): Neural Dynamics of Autistic Repetitive Behaviors and Fragile X Syndrome: Basal Ganglia Movement Gating and mGluR-Modulated Adaptively Timed Learning. Frontiers in psychology. 9:269. [PubMed: 29593596]
13. Ade KK, Wan Y, Hamann HC, O'Hare JK, Guo W, Quian A, et al. (2016): Increased Metabotropic Glutamate Receptor 5 Signaling Underlies Obsessive-Compulsive Disorder-like Behavioral and Striatal Circuit Abnormalities in Mice. Biol Psychiatry. 80:522–533. [PubMed: 27436084]
14. O'Hare JK, Ade KK, Sukharnikova T, Van Hooser SD, Palmeri ML, Yin HH, et al. (2016): Pathway-Specific Striatal Substrates for Habitual Behavior. Neuron. 89:472–479. [PubMed: 26804995]
15. Rothwell PE, Fuccillo MV, Maxeiner S, Hayton SJ, Gokce O, Lim BK, et al. (2014): Autism-associated neuroligin-3 mutations commonly impair striatal circuits to boost repetitive behaviors. Cell. 158:198–212. [PubMed: 24995986]
16. Rothwell PE, Hayton SJ, Sun GL, Fuccillo MV, Lim BK, Malenka RC (2015): Input-and output-specific regulation of serial order performance by corticostriatal circuits. Neuron. 88:345–356. [PubMed: 26494279]
17. Sheng MJ, Lu D, Shen ZM, Poo MM (2019): Emergence of stable striatal D1R and D2R neuronal ensembles with distinct firing sequence during motor learning. Proceedings of the National Academy of Sciences of the United States of America.
18. Wang W, Li C, Chen Q, van der Goes MS, Hawrot J, Yao AY, et al. (2017): Striatopallidal dysfunction underlies repetitive behavior in Shank3-deficient model of autism. J Clin Invest. 127:1978–1990. [PubMed: 28414301]
19. Wang X, Bey AL, Katz BM, Badea A, Kim N, David LK, et al. (2016): Altered mGluR5-Homer scaffolds and corticostriatal connectivity in a Shank3 complete knockout model of autism. Nature communications. 7:11459.
20. Gerfen CR, Surmeier DJ (2011): Modulation of striatal projection systems by dopamine. Annual review of neuroscience. 34:441–466.

21. Cui G, Jun SB, Jin X, Pham MD, Vogel SS, Lovinger DM, et al. (2013): Concurrent activation of striatal direct and indirect pathways during action initiation. Nature. 494:238–242. [PubMed: 23354054]
22. Tecuapetla F, Matias S, Dugue GP, Mainen ZF, Costa RM (2014): Balanced activity in basal ganglia projection pathways is critical for contraversive movements. Nature communications. 5:4315.
23. Trusel M, Cavaccini A, Gritti M, Greco B, Saintot PP, Nazzaro C, et al. (2015): Coordinated Regulation of Synaptic Plasticity at Striatopallidal and Striatonigral Neurons Orchestrates Motor Control. Cell Rep. 13:1353–1365. [PubMed: 26549453]
24. Corbit LH, Muir JL, Balleine BW (2003): Lesions of mediodorsal thalamus and anterior thalamic nuclei produce dissociable effects on instrumental conditioning in rats. The European journal of neuroscience. 18:1286–1294. [PubMed: 12956727]
25. Gerfen CR, Engber TM, Mahan LC, Susel Z, Chase TN, Monsma FJ, et al. (1990): D1 and D2 dopamine receptor-regulated gene expression of striatonigral and striatopallidal neurons. Science. 250:1429–1432. [PubMed: 2147780]
26. Greengard P (2001): The neurobiology of slow synaptic transmission. Science. 294:1024–1030. [PubMed: 11691979]
27. Uematsu K, Heiman M, Zelenina M, Padovan J, Chait BT, Aperia A, et al. (2015): Protein kinase A directly phosphorylates metabotropic glutamate receptor 5 to modulate its function. J Neurochem. 132:677–686. [PubMed: 25639954]
28. Voulalas PJ, Holtzclaw L, Wolstenholme J, Russell JT, Hyman SE (2005): Metabotropic glutamate receptors and dopamine receptors cooperate to enhance extracellular signal-regulated kinase phosphorylation in striatal neurons. J Neurosci. 25:3763–3773. [PubMed: 15829628]
29. Francesconi A, Duvoisin RM (2000): Opposing effects of protein kinase C and protein kinase A on metabotropic glutamate receptor signaling: selective desensitization of the inositol trisphosphate/Ca2+ pathway by phosphorylation of the receptor-G protein-coupling domain. Proceedings of the National Academy of Sciences of the United States of America. 97:6185–6190. [PubMed: 10823959]
30. Martiros N, Burgess AA, Graybiel AM (2018): Inversely Active Striatal Projection Neurons and Interneurons Selectively Delimit Useful Behavioral Sequences. Curr Biol. 28:560–573.e565. [PubMed: 29429614]
31. Barnes TD, Kubota Y, Hu D, Jin DZ, Graybiel AM (2005): Activity of striatal neurons reflects dynamic encoding and recoding of procedural memories. Nature. 437:1158–1161. [PubMed: 16237445]
32. Jin X, Costa RM (2010): Start/stop signals emerge in nigrostriatal circuits during sequence learning. Nature. 466:457–462. [PubMed: 20651684]
33. Jin X, Tecuapetla F, Costa RM (2014): Basal ganglia subcircuits distinctively encode the parsing and concatenation of action sequences. Nat Neurosci. 17:423–430. [PubMed: 24464039]
34. Jog MS, Kubota Y, Connolly CI, Hillegaart V, Graybiel AM (1999): Building neural representations of habits. Science. 286:1745–1749. [PubMed: 10576743]
35. Gillan CM, Morein-Zamir S, Kaser M, Fineberg NA, Sule A, Sahakian BJ, et al. (2014): Counterfactual processing of economic action-outcome alternatives in obsessive-compulsive disorder: further evidence of impaired goal-directed behavior. Biol Psychiatry. 75:639–646. [PubMed: 23452663]
36. Gillan CM, Morein-Zamir S, Urcelay GP, Sule A, Voon V, Apergis-Schoute AM, et al. (2014): Enhanced avoidance habits in obsessive-compulsive disorder. Biol Psychiatry. 75:631–638. [PubMed: 23510580]
37. D'Antoni S, Spatuzza M, Bonaccorso CM, Musumeci SA, Ciranna L, Nicoletti F, et al. (2014): Dysregulation of group-I metabotropic glutamate (mGlu) receptor mediated signalling in disorders associated with Intellectual Disability and Autism. Neuroscience and biobehavioral reviews. 46 Pt 2:228–241. [PubMed: 24548786]
38. Matosin N, Fernandez-Enright F, Lum JS, Newell KA (2017): Shifting towards a model of mGluR5 dysregulation in schizophrenia: consequences for future schizophrenia treatment. Neuropharmacology. 115:73–91. [PubMed: 26349010]

39. Mehta MV, Gandal MJ, Siegel SJ (2011): mGluR5-antagonist mediated reversal of elevated stereotyped, repetitive behaviors in the VPA model of autism. PLoS One. 6:e26077. [PubMed: 22016815]
40. Pop AS, Gomez-Mancilla B, Neri G, Willemsen R, Gasparini F (2014): Fragile X syndrome: a preclinical review on metabotropic glutamate receptor 5 (mGluR5) antagonists and drug development. Psychopharmacology (Berl). 231:1217–1226. [PubMed: 24232444]
41. Stewart SE, Yu D, Scharf JM, Neale BM, Fagerness JA, Mathews CA, et al. (2013): Genome-wide association study of obsessive-compulsive disorder. Molecular Psychiatry. 18:788–798. [PubMed: 22889921]
42. Ronesi JA, Collins KA, Hays SA, Tsai NP, Guo W, Birnbaum SG, et al. (2012): Disrupted Homer scaffolds mediate abnormal mGluR5 function in a mouse model of fragile X syndrome. Nat Neurosci. 15:431–440, s431. [PubMed: 22267161]
43. Bienvenu OJ, Wang Y, Shugart YY, Welch JM, Grados MA, Fyer AJ, et al. (2009): Sapap3 and pathological grooming in humans: Results from the OCD collaborative genetics study. Am J Med Genet B Neuropsychiatr Genet. 150B:710–720. [PubMed: 19051237]
44. Naaz S, Balachander S, Srinivasa Murthy N, Ms B, Sud R, Saha P, et al. (2020): Association of SAPAP3 allelic variants with symptom dimensions and pharmacological treatment response in obsessive-compulsive disorder. Exp Clin Psychopharmacol.
45. Zuchner S, Wendland JR, Ashley-Koch AE, Collins AL, Tran-Viet KN, Quinn K, et al. (2009): Multiple rare SAPAP3 missense variants in trichotillomania and OCD. Mol Psychiatry. 14:6–9. [PubMed: 19096451]
46. Chen M, Wan Y, Ade K, Ting J, Feng G, Calakos N (2011): Sapap3 deletion anomalously activates short-term endocannabinoid-mediated synaptic plasticity. J Neurosci. 31:9563–9573. [PubMed: 21715621]
47. Corbit VL, Manning EE, Gittis AH, Ahmari SE (2019): Strengthened Inputs from Secondary Motor Cortex to Striatum in a Mouse Model of Compulsive Behavior. J Neurosci. 39:2965–2975. [PubMed: 30737313]
48. Hadjas LC, Lüscher C, Simmler LD (2019): Aberrant habit formation in the Sapap3-knockout mouse model of obsessive-compulsive disorder. Sci Rep. 9:12061. [PubMed: 31427755]
49. Hadjas LC, Schartner MM, Cand J, Creed MC, Pascoli V, Luscher C, et al. (2020): Projection-specific deficits in synaptic transmission in adult Sapap3-knockout mice. Neuropsychopharmacology : official publication of the American College of Neuropsychopharmacology.
50. Wan Y, Ade KK, Caffall Z, Ilcim Ozlu M, Eroglu C, Feng G, et al. (2014): Circuit-selective striatal synaptic dysfunction in the Sapap3 knockout mouse model of obsessive-compulsive disorder. Biol Psychiatry. 75:623–630. [PubMed: 23414593]
51. Wan Y, Feng G, Calakos N (2011): Sapap3 deletion causes mGluR5-dependent silencing of AMPAR synapses. J Neurosci. 31:16685–16691. [PubMed: 22090495]
52. Welch JM, Lu J, Rodriguiz RM, Trotta NC, Peca J, Ding JD, et al. (2007): Cortico-striatal synaptic defects and OCD-like behaviours in Sapap3-mutant mice. Nature. 448:894–900. [PubMed: 17713528]
53. Kalueff AV, Stewart AM, Song C, Berridge KC, Graybiel AM, Fentress JC (2016): Neurobiology of rodent self-grooming and its value for translational neuroscience. Nature reviews Neuroscience. 17:45–59. [PubMed: 26675822]
54. Gereau RWt Heinemann SF (1998): Role of protein kinase C phosphorylation in rapid desensitization of metabotropic glutamate receptor 5. Neuron. 20:143–151. [PubMed: 9459450]
55. Ko SJ, Isozaki K, Kim I, Lee JH, Cho HJ, Sohn SY, et al. (2012): PKC phosphorylation regulates mGluR5 trafficking by enhancing binding of Siah-1A. J Neurosci. 32:16391–16401. [PubMed: 23152621]
56. Alagarsamy S, Sorensen SD, Conn PJ (2001): Coordinate regulation of metabotropic glutamate receptors. Curr Opin Neurobiol. 11:357–362. [PubMed: 11399435]
57. Kliewer A, Reinscheid RK, Schulz S (2017): Emerging Paradigms of G Protein-Coupled Receptor Dephosphorylation. Trends Pharmacol Sci. 38:621–636. [PubMed: 28478994]

58. Cohen PT (2002): Protein phosphatase 1--targeted in many directions. J Cell Sci. 115:241–256. [PubMed: 11839776]
59. Allen PB, Ouimet CC, Greengard P (1997): Spinophilin, a novel protein phosphatase 1 binding protein localized to dendritic spines. Proc Natl Acad Sci U S A. 94:9956–9961. [PubMed: 9275233]
60. Colbran RJ, Bass MA, McNeill RB, Bollen M, Zhao S, Wadzinski BE, et al. (1997): Association of brain protein phosphatase 1 with cytoskeletal targeting/regulatory subunits. J Neurochem. 69:920–929. [PubMed: 9282913]
61. Ragusa MJ, Dancheck B, Critton DA, Nairn AC, Page R, Peti W (2010): Spinophilin directs protein phosphatase 1 specificity by blocking substrate binding sites. Nat Struct Mol Biol. 17:459–464. [PubMed: 20305656]
62. Baucum AJ 2nd, Jalan-Sakrikar N, Jiao Y, Gustin RM, Carmody LC, Tabb DL, et al. (2010): Identification and validation of novel spinophilin-associated proteins in rodent striatum using an enhanced ex vivo shotgun proteomics approach. Mol Cell Proteomics. 9:1243–1259. [PubMed: 20124353]
63. Sarrouilhe D, di Tommaso A, Metaye T, Ladeveze V (2006): Spinophilin: from partners to functions. Biochimie. 88:1099–1113. [PubMed: 16737766]
64. Watkins DS, True JD, Mosley AL, Baucum AJ 2nd (2018): Proteomic Analysis of the Spinophilin Interactome in Rodent Striatum Following Psychostimulant Sensitization. Proteomes. 6.
65. Allen PB, Zachariou V, Svenningsson P, Lepore AC, Centonze D, Costa C, et al. (2006): Distinct roles for spinophilin and neurabin in dopamine-mediated plasticity. Neuroscience. 140:897–911. [PubMed: 16600521]
66. Edler MC, Salek AB, Watkins DS, Kaur H, Morris CW, Yamamoto BK, et al. (2018): Mechanisms Regulating the Association of Protein Phosphatase 1 with Spinophilin and Neurabin. ACS Chem Neurosci. 9:2701–2712. [PubMed: 29786422]
67. Morris CW, Watkins DS, Salek AB, Edler MC, Baucum AJ 2nd (2018): The association of spinophilin with disks large-associated protein 3 (SAPAP3) is regulated by metabotropic glutamate receptor (mGluR) 5. Molecular and cellular neurosciences. 90:60–69. [PubMed: 29908232]
68. Areal LB, Hamilton A, Martins-Silva C, Pires RGW, Ferguson SSG (2019): Neuronal scaffolding protein spinophilin is integral for cocaine-induced behavioral sensitization and ERK1/2 activation. Mol Brain. 12:15. [PubMed: 30803445]
69. Di Sebastiano AR, Fahim S, Dunn HA, Walther C, Ribeiro FM, Cregan SP, et al. (2016): Role of Spinophilin in Group I Metabotropic Glutamate Receptor Endocytosis, Signaling, and Synaptic Plasticity. J Biol Chem. 291:17602–17615. [PubMed: 27358397]
70. Fujii S, Yamazoe G, Itoh M, Kubo Y, Saitoh O (2008): Spinophilin inhibits the binding of RGS8 to M1-mAChR but enhances the regulatory function of RGS8. Biochemical and biophysical research communications. 377:200–204. [PubMed: 18834863]
71. Kurogi M, Nagatomo K, Kubo Y, Saitoh O (2009): Effects of spinophilin on the function of RGS8 regulating signals from M2 and M3-mAChRs. Neuroreport. 20:1134–1139. [PubMed: 19609226]
72. Wang Q, Zhao J, Brady AE, Feng J, Allen PB, Lefkowitz RJ, et al. (2004): Spinophilin blocks arrestin actions in vitro and in vivo at G protein-coupled receptors. Science (New York, NY. 304:1940–1944.
73. Wang X, Zeng W, Kim MS, Allen PB, Greengard P, Muallem S (2007): Spinophilin/neurabin reciprocally regulate signaling intensity by G protein-coupled receptors. The EMBO journal. 26:2768–2776. [PubMed: 17464283]
74. Wang X, Zeng W, Soyombo AA, Tang W, Ross EM, Barnes AP, et al. (2005): Spinophilin regulates Ca2+ signalling by binding the N-terminal domain of RGS2 and the third intracellular loop of G-protein-coupled receptors. Nat Cell Biol. 7:405–411. [PubMed: 15793568]
75. Karahan H, Smith DC, Kim B, Dabin LC, Al-Amin MM, Wijeratne HRS, et al. (2021): Deletion of Abi3 gene locus exacerbates neuropathological features of Alzheimer's disease in a mouse model of Aβ amyloidosis. Sci Adv. 7:eabe3954. [PubMed: 34731000]
76. Yin HH, Mulcare SP, Hilario MR, Clouse E, Holloway T, Davis MI, et al. (2009): Dynamic reorganization of striatal circuits during the acquisition and consolidation of a skill. Nat Neurosci. 12:333–341. [PubMed: 19198605]

77. Salek AB, Edler MC, McBride JP, Baucum AJ, 2nd (2019): Spinophilin regulates phosphorylation and interactions of the GluN2B subunit of the N-methyl-d-aspartate receptor. J Neurochem. 151:185–203. [PubMed: 31325175]

78. Hiday AC, Edler MC, Salek AB, Morris CW, Thang M, Rentz TJ, et al. (2017): Mechanisms and Consequences of Dopamine Depletion-Induced Attenuation of the Spinophilin/Neurofilament Medium Interaction. Neural Plast. 2017:4153076. [PubMed: 28634551]

79. Grecco GG, Haggerty DL, Doud EH, Fritz BM, Yin F, Hoffman H, et al. (2021): A multi-omic analysis of the dorsal striatum in an animal model of divergent genetic risk for alcohol use disorder. J Neurochem. 157:1013–1031. [PubMed: 33111353]

80. Muhammad K, Reddy-Alla S, Driller JH, Schreiner D, Rey U, Bohme MA, et al. (2015): Presynaptic spinophilin tunes neurexin signalling to control active zone architecture and function. Nat Commun. 6:8362. [PubMed: 26471740]

81. Muly EC, Allen P, Mazloom M, Aranbayeva Z, Greenfield AT, Greengard P (2004): Subcellular distribution of neurabin immunolabeling in primate prefrontal cortex: comparison with spinophilin. Cereb Cortex. 14:1398–1407. [PubMed: 15217898]

82. Ouimet CC, Katona I, Allen P, Freund TF, Greengard P (2004): Cellular and subcellular distribution of spinophilin, a PP1 regulatory protein that bundles F-actin in dendritic spines. The Journal of comparative neurology. 479:374–388. [PubMed: 15514983]

83. Kreitzer AC, Malenka RC (2005): Dopamine modulation of state-dependent endocannabinoid release and long-term depression in the striatum. Journal of Neuroscience. 25:10537–10545. [PubMed: 16280591]

84. Wu Y-W, Kim J-I, Tawfik Vivianne L, Lalchandani Rupa R, Scherrer G, Ding Jun B (2015): Input- and Cell-Type-Specific Endocannabinoid-Dependent LTD in the Striatum. Cell Reports. 10:75–87. [PubMed: 25543142]

85. Smith FD, Oxford GS, Milgram SL (1999): Association of the D2 dopamine receptor third cytoplasmic loop with spinophilin, a protein phosphatase-1-interacting protein. The Journal of biological chemistry. 274:19894–19900. [PubMed: 10391935]

86. Berridge KC, Aldridge JW (2000): Super-stereotypy I: enhancement of a complex movement sequence by systemic dopamine D1 agonists. Synapse. 37:194–204. [PubMed: 10881041]

87. Stein BD, Herzig S, Martínez-Bartolomé S, Lavallée-Adam M, Shaw RJ, Yates JR (2019): Comparison of CRISPR Genomic Tagging for Affinity Purification and Endogenous Immunoprecipitation Coupled with Quantitative Mass Spectrometry To Identify the Dynamic AMPKα2 Interactome. Journal of Proteome Research. 18:3703–3714. [PubMed: 31398040]

88. Wu K, Hanna GL, Easter P, Kennedy JL, Rosenberg DR, Arnold PD (2013): Glutamate system genes and brain volume alterations in pediatric obsessive-compulsive disorder: a preliminary study. Psychiatry Res. 211:214–220. [PubMed: 23154099]

89. Durand CM, Betancur C, Boeckers TM, Bockmann J, Chaste P, Fauchereau F, et al. (2007): Mutations in the gene encoding the synaptic scaffolding protein SHANK3 are associated with autism spectrum disorders. Nature Genetics. 39:25–27. [PubMed: 17173049]

90. Prasad C, Prasad AN, Chodirker BN, Lee C, Dawson AK, Jocelyn LJ, et al. (2000): Genetic evaluation of pervasive developmental disorders: the terminal 22q13 deletion syndrome may represent a recognizable phenotype. Clinical Genetics. 57:103–109. [PubMed: 10735630]

91. Wilson HL, Wong ACC, Shaw SR, Tse W-Y, Stapleton GA, Phelan MC, et al. (2003): Molecular characterisation of the 22q13 deletion syndrome supports the role of haploinsufficiency of SHANK3/PROSAP2 in the major neurological symptoms. Journal of Medical Genetics. 40:575–584. [PubMed: 12920066]

92. Chien W-H, Gau S-F, Liao H-M, Chiu Y-N, Wu Y-Y, Huang Y-S, et al. (2013): Deep exon resequencing of DLGAP2 as a candidate gene of autism spectrum disorders. Molecular Autism. 4:26. [PubMed: 23915500]

93. Marshall CR, Noor A, Vincent JB, Lionel AC, Feuk L, Skaug J, et al. (2008): Structural Variation of Chromosomes in Autism Spectrum Disorder. The American Journal of Human Genetics. 82:477–488. [PubMed: 18252227]

94. Pinto D, Pagnamenta AT, Klei L, Anney R, Merico D, Regan R, et al. (2010): Functional impact of global rare copy number variation in autism spectrum disorders. Nature. 466:368–372. [PubMed: 20531469]

95. Um JW, Ko J (2017): Neural Glycosylphosphatidylinositol-Anchored Proteins in Synaptic Specification. Trends Cell Biol. 27:931–945. [PubMed: 28743494]

96. Ramírez-Armenta KI, Alatriste-León H, Verma-Rodríguez AK, Llanos-Moreno A, Ramírez-Jarquín JO, Tecuapetla F (2022): Optogenetic inhibition of indirect pathway neurons in the dorsomedial striatum reduces excessive grooming in Sapap3-knockout mice. Neuropsychopharmacology : official publication of the American College of Neuropsychopharmacology. 47:477–487. [PubMed: 34417544]

97. Noetzel MJ, Rook JM, Vinson PN, Cho HP, Days E, Zhou Y, et al. (2012): Functional impact of allosteric agonist activity of selective positive allosteric modulators of metabotropic glutamate receptor subtype 5 in regulating central nervous system function. Mol Pharmacol. 81:120–133. [PubMed: 22021324]

98. Notartomaso S, Zappulla C, Biagioni F, Cannella M, Bucci D, Mascio G, et al. (2013): Pharmacological enhancement of mGlu1 metabotropic glutamate receptors causes a prolonged symptomatic benefit in a mouse model of spinocerebellar ataxia type 1. Molecular Brain. 6:48. [PubMed: 24252411]

99. Zuena AR, Iacovelli L, Orlando R, Di Menna L, Casolini P, Alemà GS, et al. (2018): In Vivo Nonradioactive Assessment of mGlu5 Receptor-Activated Polyphosphoinositide Hydrolysis in Response to Systemic Administration of a Positive Allosteric Modulator. Frontiers In pharmacology. 9.

100. Berridge KC, Aldridge JW (2000): Super-stereotypy II: enhancement of a complex movement sequence by intraventricular dopamine D1 agonists. Synapse. 37:205–215. [PubMed: 10881042]

101. Augustin SM, Loewinger GC, O'Neal TJ, Kravitz AV, Lovinger DM (2020): Dopamine D2 receptor signaling on iMSNs is required for initiation and vigor of learned actions. Neuropsychopharmacology : official publication of the American College of Neuropsychopharmacology. 45:2087–2097. [PubMed: 32811899]

102. Peca J, Feliciano C, Ting JT, Wang W, Wells MF, Venkatraman TN, et al. (2011): Shank3 mutant mice display autistic-like behaviours and striatal dysfunction. Nature. 472:437–442. [PubMed: 21423165]

103. Raka F, Di Sebastiano AR, Kulhawy SC, Ribeiro FM, Godin CM, Caetano FA, et al. (2015): Ca2+/Calmodulin-dependent protein Kinase II interacts with group I Metabotropic Glutamate and facilitates Receptor Endocytosis and ERK1/2 signaling: role of β-Amyloid. Molecular Brain. 8:21. [PubMed: 25885040]

104. Kim CH, Braud S, Isaac JT, Roche KW (2005): Protein kinase C phosphorylation of the metabotropic glutamate receptor mGluR5 on Serine 839 regulates Ca2+ oscillations. J Biol Chem. 280:25409–25415. [PubMed: 15894802]

105. Lee JH, Lee J, Choi KY, Hepp R, Lee JY, Lim MK, et al. (2008): Calmodulin dynamically regulates the trafficking of the metabotropic glutamate receptor mGluR5. Proceedings of the National Academy of Sciences of the United States of America. 105:12575–12580. [PubMed: 18715999]

106. Kalinowska M, Castillo C, Francesconi A (2015): Quantitative Profiling of Brain Lipid Raft Proteome in a Mouse Model of Fragile X Syndrome. PLOS ONE. 10:e0121464. [PubMed: 25849048]

107. Toupin A, Benachenhou S, Abolghasemi A, Laroui A, Galarneau L, Fülöp T, et al. (2022): Association of lipid rafts cholesterol with clinical profile in fragile X syndrome. Scientific Reports. 12:2936. [PubMed: 35190617]

108. Wang H (2014): Lipid rafts: a signaling platform linking cholesterol metabolism to synaptic deficits in autism spectrum disorders. Frontiers in behavioral neuroscience. 8:104. [PubMed: 24723866]

109. Francesconi A, Kumari R, Zukin RS (2009): Regulation of group I metabotropic glutamate receptor trafficking and signaling by the caveolar/lipid raft pathway. J Neurosci. 29:3590–3602. [PubMed: 19295163]

110. Mao L, Yang L, Tang Q, Samdani S, Zhang G, Wang JQ (2005): The scaffold protein Homer1b/c links metabotropic glutamate receptor 5 to extracellular signal-regulated protein kinase cascades in neurons. J Neurosci. 25:2741–2752. [PubMed: 15758184]

111. Tu JC, Xiao B, Yuan JP, Lanahan AA, Leoffert K, Li M, et al. (1998): Homer binds a novel proline-rich motif and links group 1 metabotropic glutamate receptors with IP3 receptors. Neuron. 21:717–726. [PubMed: 9808459]

112. Mink JW (1996): The basal ganglia: focused selection and inhibition of competing motor programs. Prog Neurobiol. 50:381–425. [PubMed: 9004351]

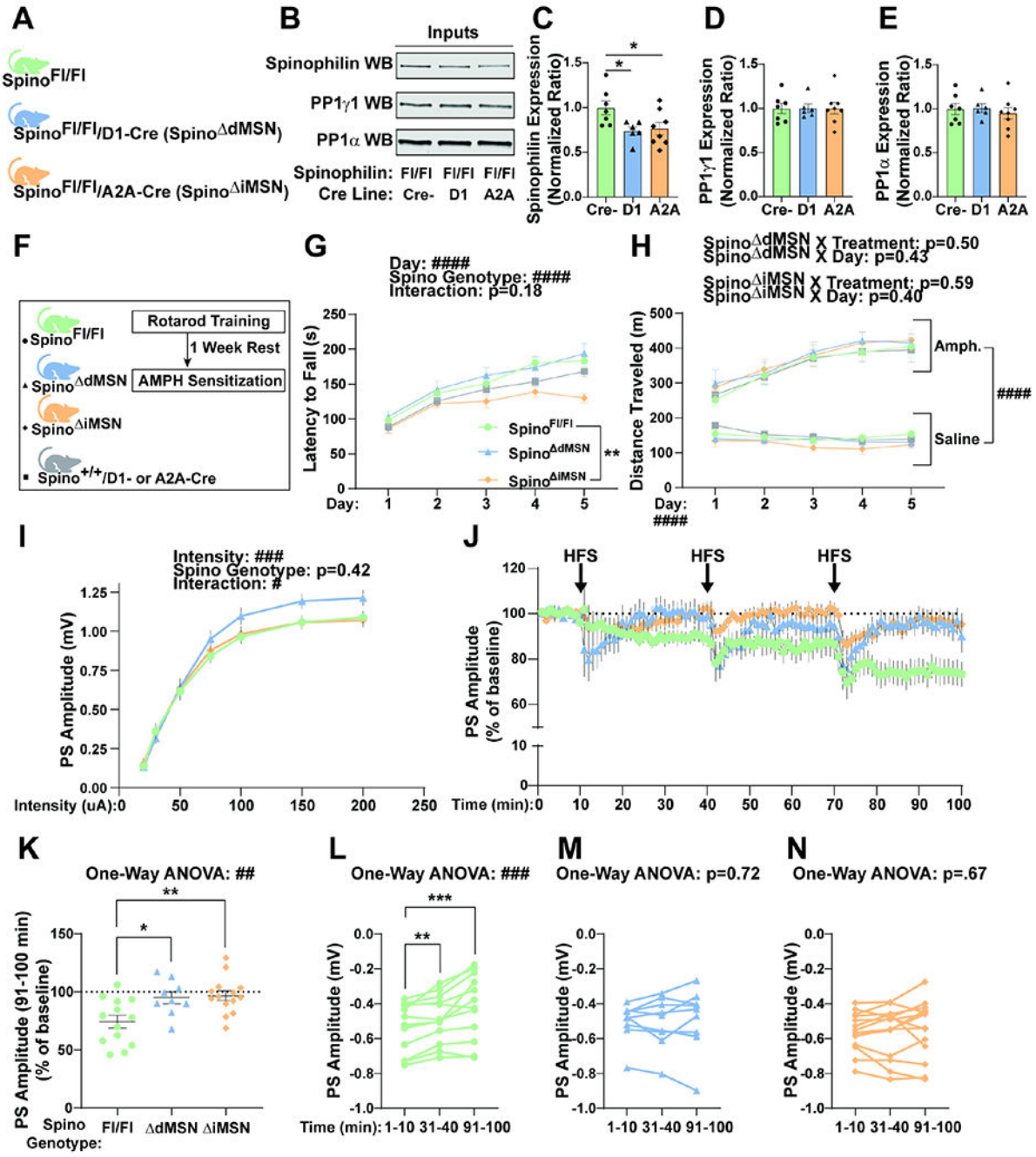


**Figure 1: Spinophilin has MSN subtype-specific roles in mediating motor function and striatal plasticity.**

**A)** Conditional spinophilin mice ($Spino^{Fl/Fl}$) were crossed with Cre constitutively expressed under the Drd1 (D1)- or Adora2a (A2A)- promotor to deplete spinophilin expression in dMSNs ($Spino^{\Delta dMSN}$) or iMSNs ($Spino^{\Delta iMSN}$), respectively. At 2-4 months of age, 2 mm striatal punches were taken from coronal slices isolated from male or female mice for **B)** immunoblot analysis of spinophilin and PP1 protein expression. One-way ANOVA with post-hoc Dunnett's multiple comparisons test detected a significant decrease in **C)**

spinophilin expression in Spino$^{\Delta dMSN}$ and Spino$^{\Delta iMSN}$ compared to control (p=0.032 and p=0.041, respectively). There was no change in **D)** PP1γ1 (p=0.99) or **E)** PP1α (p=0.75) expression. N=8 Spino$^{Fl/Fl}$ (6 male), 6 Spino$^{\Delta dMSN}$ (2 male), 7 Spino$^{\Delta iMSN}$ (4 male). **F)** 7-9 week-old control and MSN subtype-specific spinophilin KO mice were trained on accelerating rotarod for 5-days. After one week of rest, these same animals were treated with a sensitizing regimen of d-amphetamine (3 mg/kg) for 5-days. **G)** Two-way ANOVA with repeated measures and post-hoc Dunnett's multiple comparisons test determined Spino$^{\Delta iMSN}$ mice displayed significantly worse rotarod performance than Spino$^{Fl/Fl}$ controls (p=0.002). N=17 Spino$^{Fl/Fl}$ (7 male), 17 Spino$^{+/+}$/D1- or A2A-Cre (11 male), 15 Spino$^{\Delta dMSN}$ (10 male), 15 Spino$^{\Delta iMSN}$ (5 male). **H)** Three-way ANOVAs with repeated measures detected significant day (p<0.0001) and treatment (p<0.0001) effects, but not Spino$^{\Delta dMSN}$ or Spino$^{\Delta iMSN}$ genotype or interaction effects on locomotion following 5-daily treatments with saline- or amphetamine. N=8/15 saline/AMPH-treated Spino$^{Fl/Fl}$ (2/5 male), 9/8 saline/AMPH-treated Spino$^{+/+}$/D1- or A2A-Cre (7/4 male), 6/9 saline/AMPH-treated Spino$^{\Delta dMSN}$ (5/5 male), 6/9 saline/AMPH-treated Spino$^{\Delta iMSN}$ (2/3 male). Field population spike amplitudes from the DLS were measured in response to **I)** stimulation intensity increases or **J)** high-frequency stimulations that result in long-term depression (LTD). Two-way ANOVA with repeated measures detected a spinophilin genotype X stimulation intensity interaction (p=0.02); however, post-hoc Šídák's multiple comparisons test did not detect group differences at any specific intensity. N=34 slices from 20 Spino$^{Fl/Fl}$ mice (11 male mice), 27 slices from 17 Spino$^{\Delta dMSN}$ mice (10 male mice), 28 slices from 17 Spino$^{\Delta iMSN}$ mice (10 male mice). One-way ANOVA with post-hoc Dunnett's multiple comparisons test determined that **K)** LTD is decreased in both Spino$^{\Delta dMSN}$ and Spino$^{\Delta iMSN}$ compared to control from 91-100 minutes (p=0.018 and p=0.004, respectively). One-way ANOVAs with repeated measures confirmed LTD in **L)** control at 31-40 and 91-100-minutes relative to the 1-10 minute baseline period (p=0.007 and p=0.0013, respectively); however, neither **M)** Spino$^{\Delta dMSN}$ nor **N)** Spino$^{\Delta iMSN}$ underwent LTD from 31-40 minutes (p=0.97 and p=0.99, respectively) or 91-100 minutes (p=0.81 and p=0.75, respectively). N=13 slices from 11 Spino$^{Fl/Fl}$ mice (5 male mice), 9 slices from 7 Spino$^{\Delta dMSN}$ mice (3 male mice), 14 slices from 10 Spino$^{\Delta iMSN}$ mice (5 male mice). Mean ± SEM. Significant two- or one-way ANOVA effects denoted by #p≤0.05, ##p≤0.01, ###p≤0.001, ####p<0.0001. Significant post-hoc tests denoted by *p≤0.05, **p≤0.01, ***p≤0.001.

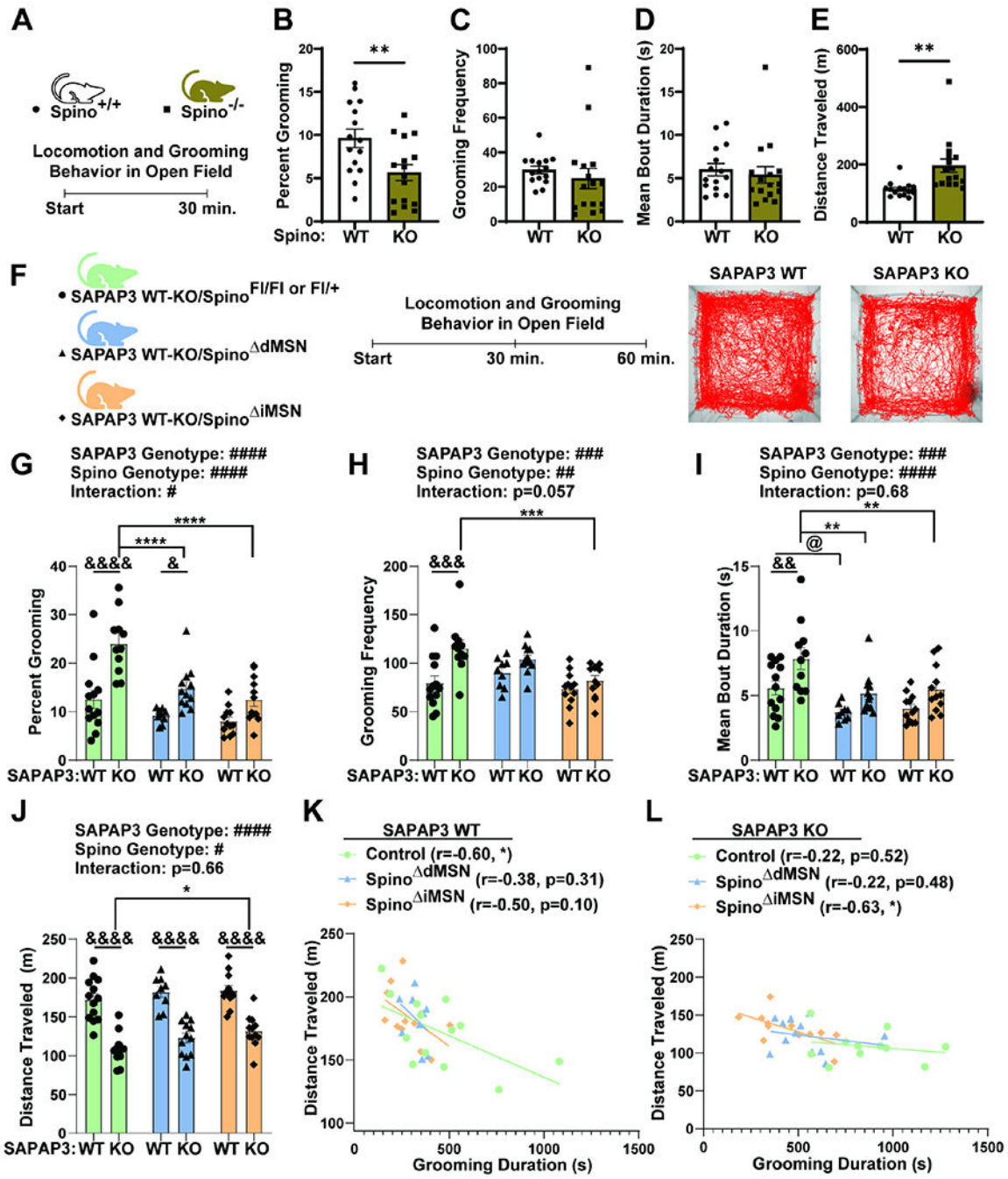


**Figure 2: MSN subtype-specific spinophilin knockout decreases excessive grooming in SAPAP3 deficient mice.**

**A)** Spinophilin wild-type (Spino$^{+/+}$) and knockout (Spino$^{-/-}$) mice were placed in the open field (OF) of Noldus Phenotyper Cages for 30 minutes at 8-weeks of age to measure locomotion and grooming behavior using the Noldus Rodent Behavior Recognition module validated in-house (Figure S10. **)B)** Unpaired t-tests determined that the percentage of time spent grooming during the recording session (percent grooming) was decreased in Spino$^{-/-}$ mice (p=0.008), but **C)** the number of grooming bouts initiated during the

session (grooming frequency) (p=0.44) nor **D)** the mean duration of individual grooming bouts throughout the session (mean bout duration) (p=0.61) was affected. **E)** Alternatively, unpaired t-test determined that Spino$^{-/-}$ mice displayed increased locomotion relative to Spino$^{+/+}$ (p=0.002). N=15 Spino$^{+/+}$ (9 male) and 16 Spino$^{-/-}$ (7 male). **F)** Double knockout mice (SAPAP3 WT and KO/spinophilin MSN subtype-specific KO) were placed in the OF of Noldus Phenotyper Cages for 60 minutes at 8-weeks of age to measure locomotion and grooming behavior as described above. Two-way ANOVAs with post-hoc Šídák's multiple comparisons tests determined: **G)** Percent grooming was significantly decreased in SAPAP3 KO/Spino$^{\Delta dMSN}$ (p<0.0001) and SAPAP3 KO/Spino$^{\Delta iMSN}$ mice (p<0.0001) compared to SAPAP3 KO control, and a significant SAPAP3 genotype effect was detected in control (p<0.0001) and Spino$^{\Delta dMSN}$ (0.039) but not Spino$^{\Delta iMSN}$ mice (p=0.10). **H)** Grooming frequency was significantly decreased in SAPAP3 KO/Spino$^{\Delta iMSN}$ compared to SAPAP3 KO control (p=0.0005), but SAPAP3 KO/Spino$^{\Delta dMSN}$ did not affect grooming frequency relative to SAPAP3 KO control (0.34). A significant SAPAP3 genotype effect was detected in control (p=0.0002), but not Spino$^{\Delta dMSN}$ (0.32) or Spino$^{\Delta iMSN}$ mice (p=0.67). **I)** Mean grooming bout duration was significantly decreased in SAPAP3 KO/Spino$^{\Delta dMSN}$ (p=0.0014) and SAPAP3 KO/Spino$^{\Delta iMSN}$ mice (p=0.004) compared to SAPAP3 KO control. A significant SAPAP3 genotype effect was detected in control (p=0.007), but not Spino$^{\Delta dMSN}$ (p=0.21) or Spino$^{\Delta iMSN}$ mice (p=0.13). **J)** Significant SAPAP3 genotype effects on distance traveled were detected in control (p<0.0001), Spino$^{\Delta dMSN}$ (p<0.0001), and Spino$^{\Delta iMSN}$ mice (p<0.0001). Distance traveled was significantly increased in SAPAP3 KO/Spino$^{\Delta iMSN}$ compared to SAPAP3 KO control (p=0.032), but SAPAP3 KO/Spino$^{\Delta dMSN}$ was not different than SAPAP3 KO control (p=0.25). Grooming duration and distance traveled from **K)** SAPAP3 WT and **L)** SAPAP3 KO groups were correlated to determine that grooming behavior negatively correlates with locomotion in SAPAP3 WT control and SAPAP3 KO/Spino$^{\Delta iMSN}$. N=11-13 SAPAP3 WT-KO/Spino$^{Fl/Fl\ or\ Fl/+}$ (7-5 male), N=9-12 SAPAP3 WT-KO/Spino$^{\Delta dMSN}$ (4-6 male), and N=12-12 SAPAP3 WT-KO/Spino$^{\Delta iMSN}$ (4-6 male). Mean ± SEM. Significant two-ANOVA effects denoted by #p≤0.05, ##p≤0.01, ###p≤0.001, ####p<0.0001. Significant post-hoc tests (Šídák's) denoted by *(Spino genotype in SAPAP3 KO), $^{@}$Spino genotype in SAPAP3 WT), and $^{\&}$(SAPAP3 WT vs SAPAP3 KO) comparisons. *p≤0.05, **p≤0.01, ***p≤0.001, ****p<0.0001.

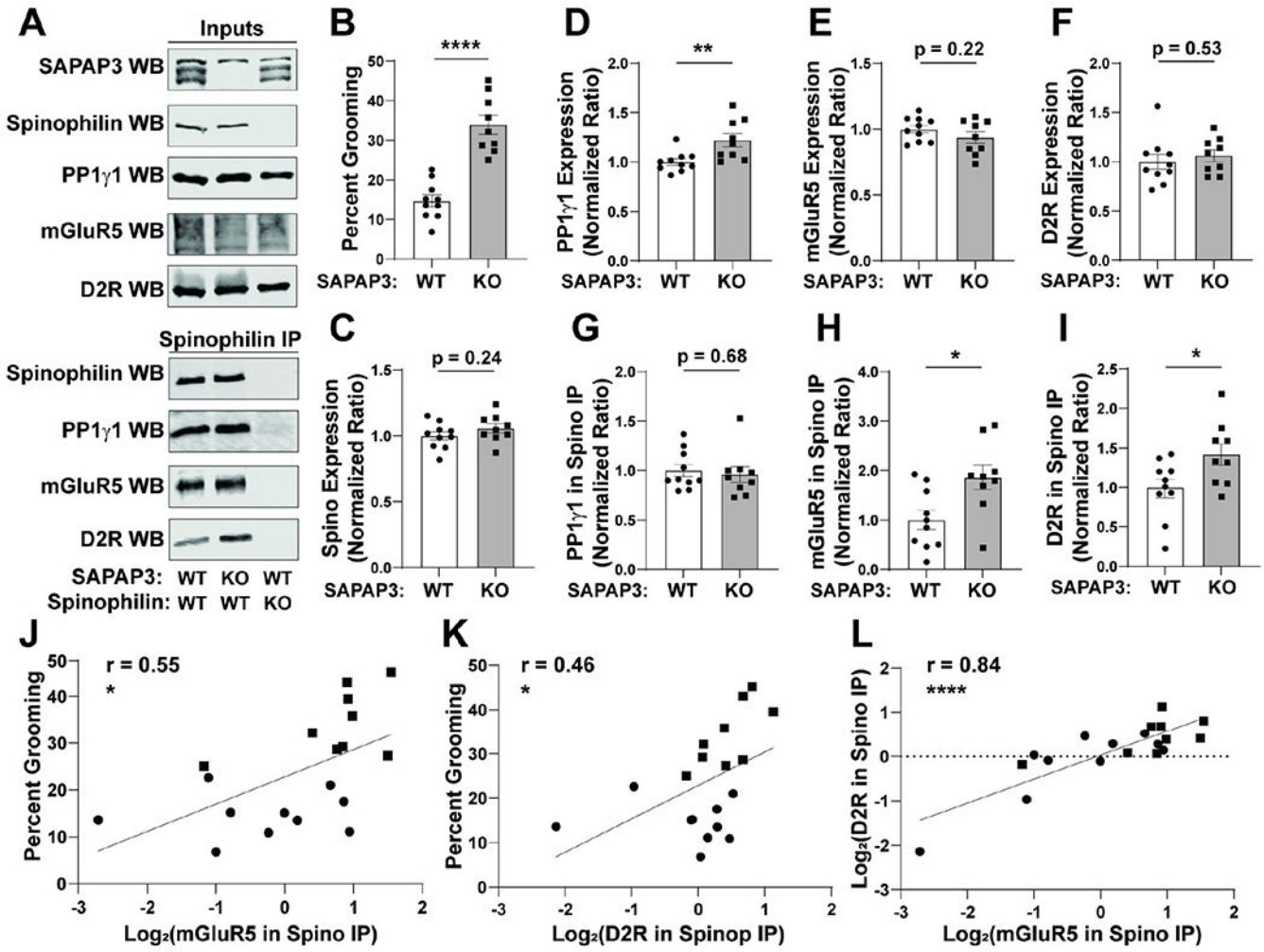


**Figure 3: Spinophilin's interactions with mGluR5 and $D_2R$ correlate with grooming behavior.**

**A-B)** The percentage of time spent grooming in 2.5 hours (percent grooming) was measured in 4-6 month-old SAPAP3 WT and KO mice ($p<0.0001$), then striatal inputs and spinophilin immunoprecipitates (IPs) were prepared for immunoblot analysis of SAPAP3, spinophilin, PP1γ1, mGluR5 and $D_2R$. Spinophilin KO striatum (lane 3) was used as a qualitative negative control to confirm the specificity of co-immunoprecipitates (co-IPs). Individual unpaired t-tests determined SAPAP3 KO did not change total protein expression of **C)** spinophilin ($p=0.24$), **E)** mGluR5 ($p=0.22$), or **F)** $D_2R$ ($p=0.53$); however, a significant increase in **D)** PP1γ1 ($p=0.007$) was determined. Analysis of IPs determined significantly more **H)** mGluR5 ($p=0.012$) and **I)** $D_2R$ ($p=0.033$) interacting with spinophilin in SAPAP3 KO striatum; however, there was no change in spinophilin's interaction with **G)** PP1γ1 ($p=0.68$). Grooming and protein interaction data from SAPAP3 WT and KO mice were pooled for Pearson's correlation analysis. Percent grooming positively correlates with spinophilin's protein interaction with **J)** mGluR5 ($r=0.556$, $p=0.013$) and **K)** $D_2R$ ($r=0.463$, $p=0.045$), and the **L)** spinophilin-mGluR5 interaction positively correlates with the spinophilin-$D_2R$ interaction ($r=0.840$, $p < 0.0001$). N=10 SAPAP3 WT (7 male) and 9 SAPAP3 KO (4 male). Mean ± SEM. *p≤0.05, **p≤0.01, ****p<0.0001.

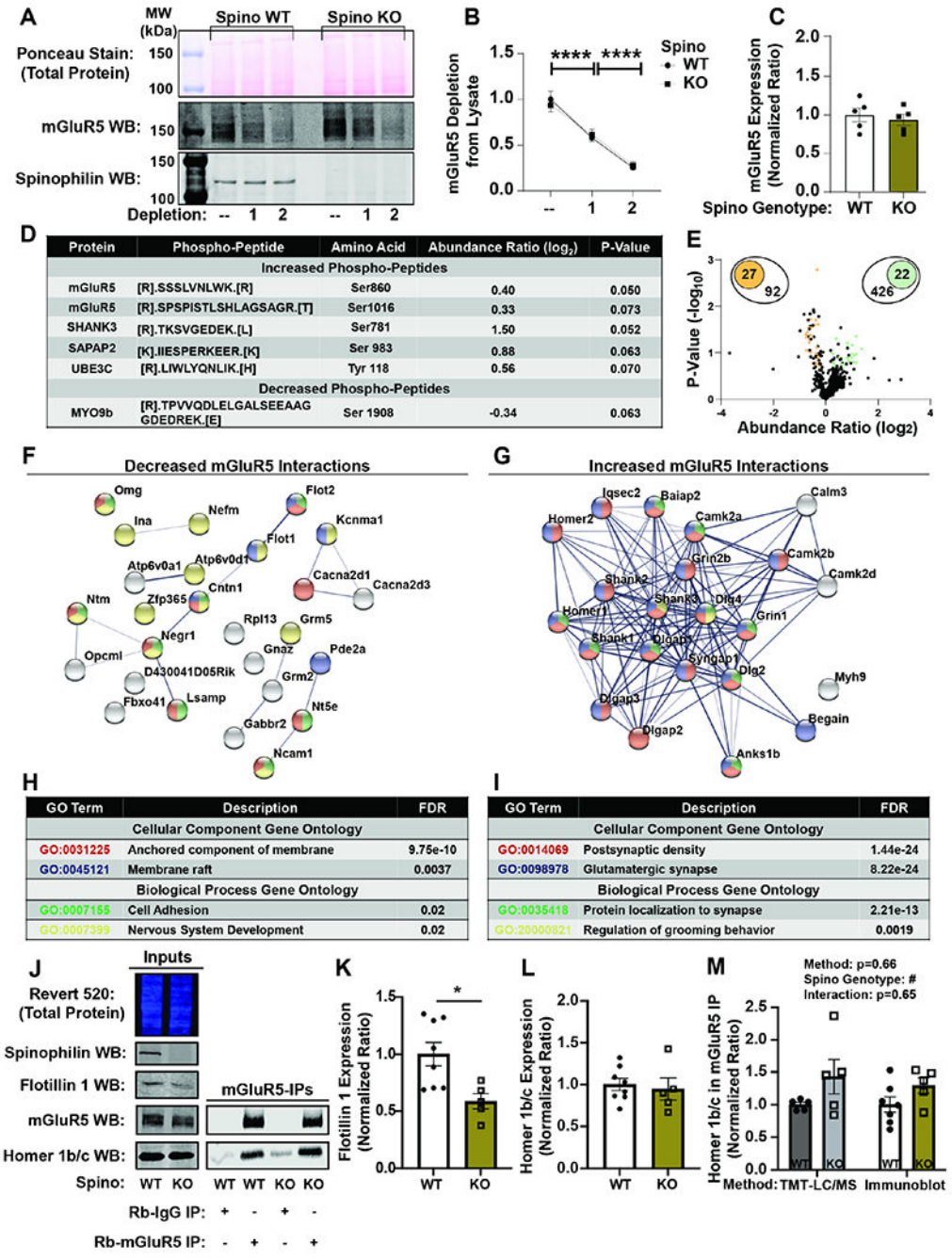


**Figure 4: Loss of spinophilin shifts mGluR5 interactions from lipid raft assemblies toward PSD proteins implicated in psychiatric disorders.**

**A)** Representative sequential mGluR5 IP from spinophilin WT (Spino$^{+/+}$) and KO (Spino$^{-/-}$) striatal lysates. We detected no difference in **B)** mGluR5 immunodepletion or **C)** mGluR5 protein expression in spino WT and KO inputs. mGluR5 IPs were submitted to the IUSM proteomics core for TMT-MS/MS analysis. **D)** Table showing increased and decreased phospho-peptides that have Abundance Ratio ($Log_2$) < −0.2 or >0.2 and one-tailed t-test p-value < 0.10. **E)** Volcano plot showing 27 decreased (orange) and 22 increased

(green) interactors having Abundance Ratio ($Log_2$) < −0.2 or >0.2, one-tailed t-test p-value < 0.10, and at least 6 unique peptides matching assigned protein. Protein-protein interaction (PPI) networks corresponding to the **F)** 27 decreased or **G)** 22 increased proteins were graphed in STRING. Graph edges correspond to proteins that participate in a function complex and edge boldness corresponds to the confidence of the interaction. Node colors correspond to gene ontology (GO) terms identified through function enrichment analysis of the **H)** decreased or **I)** increased PPI networks (false discovery rate (FDR) < 0.05). N=3 spino$^{+/+}$ (3 male) and 3 Spino$^{-/-}$ (2 male). *WT Input vs. Depletion, $^{\&}$KO Input vs Depletion. **J)** Immunoblot of flotillin 1 and homer 1b/c from spinophilin WT and KO striatal inputs and mGluR5 IPs validated that loss of spinophilin decreased **K)** flotillin-1 expression (p=0.0147). Although we found no difference in **L)** homer 1b/c expression (p=0.69), **M)** a two-way ANOVA comparing the effect method (TMT-LC/MS vs. immunoblotting) and spinophilin genotype have on the mGluR5-Homer 1b/c interaction found a significant spinophilin genotype effect (p=0.031) but no method (p=0.66) or interaction (p=0.65) effect, validating that loss of spinophilin increased mGluR5 interaction with homer1 b/c. N=7-8 Spino$^{+/+}$ (3 male) and 5 Spino$^{-/-}$ (2 male). Mean ± SEM. *p<0.05, **p<0.01, ****p<0.0001.

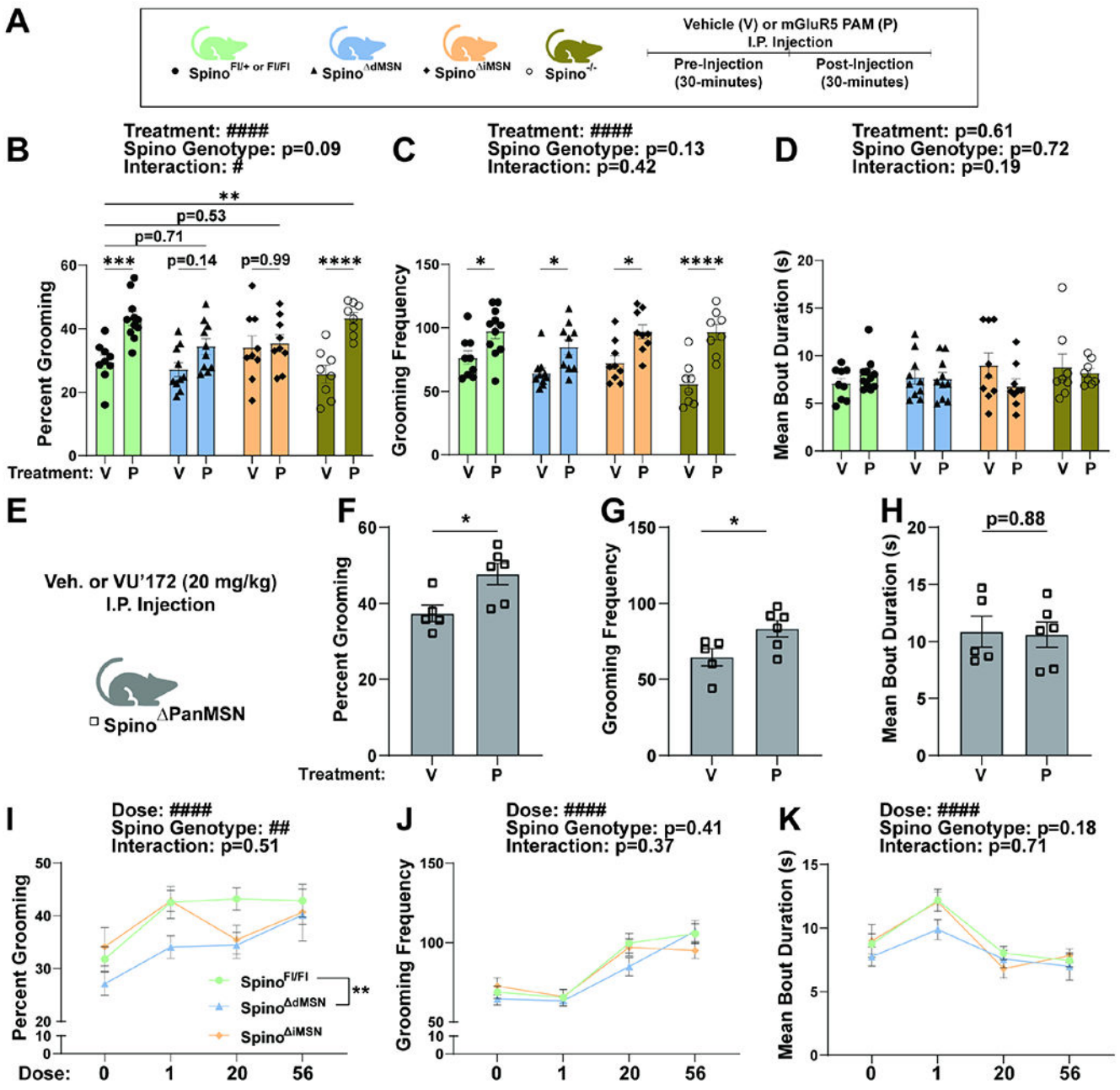


**Figure 5: Spinophilin MSN subtype-specifically decreases grooming caused by the mGluR5 PAM, VU0360172.**

**A)** Control, MSN-specific spinophilin knockout, and Spino$^{-/-}$ mice were placed in Noldus Phenotyper Cages and basal behavior (pre-injection) was measured for 30-minutes. Following a pre-injection period, mice were removed from the arena and given an I.P. injection of vehicle (V) or the mGluR5 PAM (P), VU0360172 (VU'172) (20mg/kg). Animals were placed back into the same pre-injection arena immediately following the I.P. injection and behavior was recorded for an additional 30-minutes (post-injection). Two-way ANOVAs with post-hoc Šídák's multiple comparisons tests determined a significant VU'172 treatment effect on **B)** the percentage of time spent grooming during the 30-minute

recording session (percent grooming) in control (p=0.0007) and Spino$^{-/-}$ (p<0.0001), but not Spino$^{\Delta dMSN}$ (p=0.139) or Spino$^{\Delta iMSN}$ (p=0.99) mice. Furthermore, percent grooming in the VU'172-treated Spino$^{\Delta dMSN}$ and Spino$^{\Delta iMSN}$ groups was not different from control vehicle (p=0.71 and p=0.53, respectively), whereas Spino$^{-/-}$ was significantly increased from control vehicle (p=0.002). **C)** VU'172 (20 mg/kg) increased the number of grooming bouts initiated during the 30-minute recording (grooming frequency) in control (p=0.03), Spino$^{\Delta dMSN}$ (p=0.03), Spino$^{\Delta iMSN}$ (p=0.01), and Spino$^{-/-}$ (p<0.0001). **D)** VU'172 (20 mg/kg) or spinophilin genotype did not affect the mean duration of individual grooming bouts throughout the 30-minute recording (mean bout duration). N=9V/10P Spino$^{Fl/+or\ Fl/Fl}$ (3/3 male), 10V/10P Spino$^{\Delta dMSN}$ (5/6 male), and 9V/9P Spino$^{\Delta iMSN}$ (4/4 male), 8V/8P spin$^{-/-}$; (3/4 male). **E)** Spino$^{\Delta PanMSN}$ were treated with vehicle (Veh.) or VU'172 (20 mg/kg). Student's t-tests determined that VU'172 significantly increased **F)** percent grooming (p=0.02) and **G)** grooming frequency (p=0.04), however, VU'172 did not affect **H)** mean grooming bout duration (p=0.88). **I-K)** Separate cohorts of Spino$^{Fl/Fl}$ control, Spino$^{\Delta dMSN}$, and Spino$^{\Delta iMSN}$ mice were treated with vehicle, 1, or 56 mg/kg VU'172 and combined with existing 20 mg/kg data (B-D) to generate 4-point dose response curves. Two-way ANOVAs with post-hoc Dunnett's multiple comparisons tests determined **I)** percent grooming was significantly decreased in Spino$^{\Delta dMSN}$ relative to Spino$^{Fl/Fl}$ control (p=0.004), but Spino$^{\Delta iMSN}$ was not different (0.56). However, spinophilin genotype did not significantly affect **J)** grooming frequency or **K)** mean grooming bout duration. N=11-22 Spino$^{Fl/Fl\ or\ Fl/+}$ (8-14 male), 8-11 Spino$^{\Delta dMSN}$ (4-6 male), and 9-11 Spino$^{\Delta iMSN}$ (2-5 male). Mean ± SEM. Significant two-ANOVA effects denoted by #p≤0.05 and ####p<0.0001. Significant post-hoc tests denoted by *p≤0.05, **p≤0.01, ***p≤0.001 ****p<0.0001.

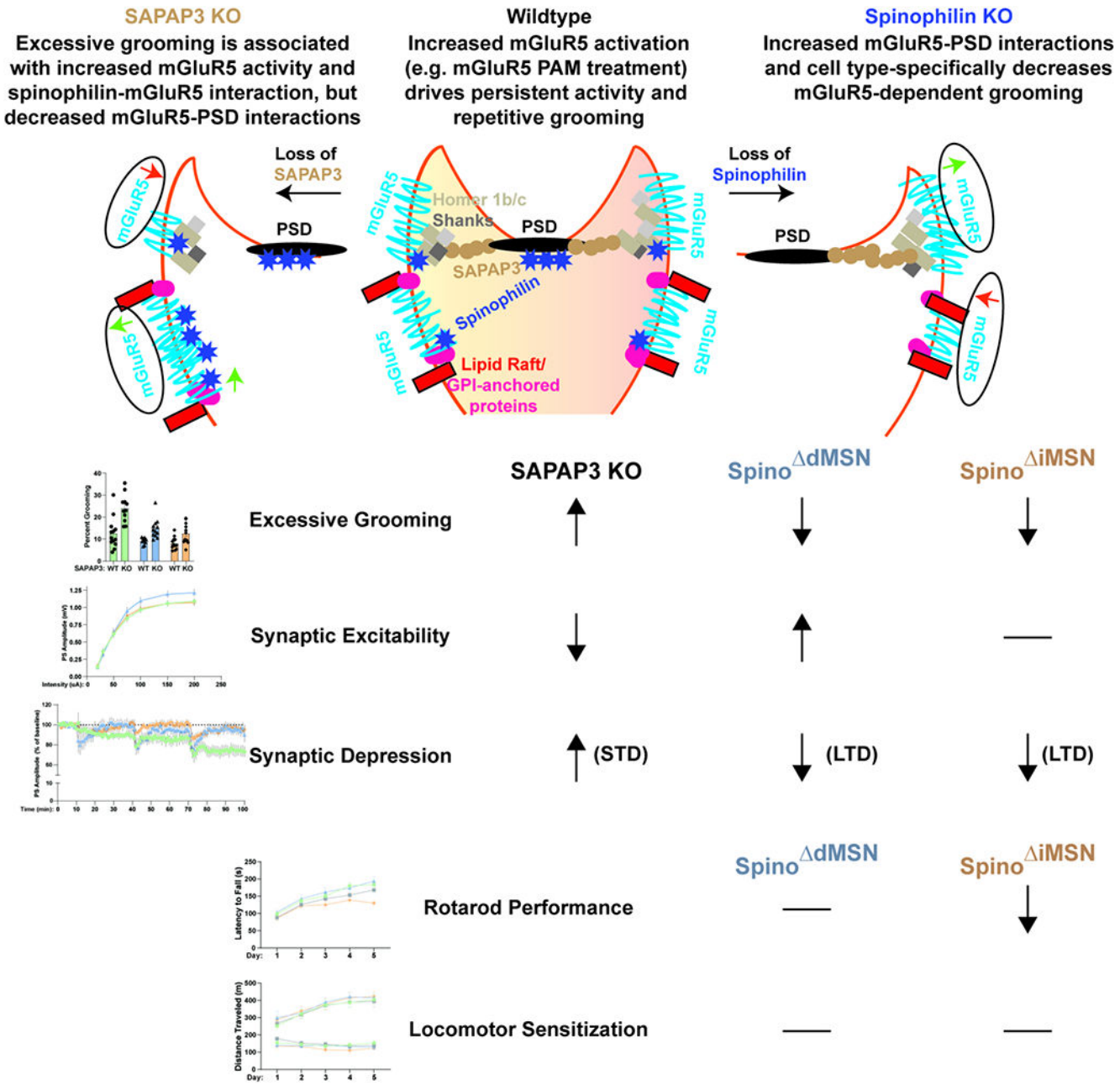


**Figure 6: Summary of protein interaction and striatal functionality changes associated with decreased mGluR5-grooming in MSN subtype-specific spinophilin knockout mice.**

Excessive grooming in SAPAP3 KO mice is associated with increased mGluR5 function and decreased mGluR5 interaction with PSD scaffolding proteins, such as homer 1b/c. Biochemically, we report more spinophilin interacts with mGluR5 in striatum of SAPAP3 KO mice and that loss of spinophilin shifts mGluR5 interactions from lipid-raft associated proteins (e.g. flotillin 1 and glycosylphosphatidylinositol (GPI)-anchored protein) toward PSD scaffolding proteins (e.g. homer 1b/c, SHANK3, and SAPAP3), suggesting spinophilin may interact with mGluR5 to maintain mGluR5-interactions with lipid raft membrane fractions—a phenotype that may facilitate pathological mGluR5 activity in SAPAP3 KO

mice. Functionally, excessive grooming in SAPAP3 KO mice is associated with decreased DLS excitability and increased DLS short-term depression (STD) (46, 52). Here, we report that decreased excessive grooming in Spino$^{\Delta dMSN}$ mice is associated with decreased duration of grooming bouts, increased DLS excitability, and decreased DLS long-term depression (LTD). Decreased excessive grooming in Spino$^{\Delta iMSN}$ mice is associated with decreased frequency and duration of grooming bouts, decreased DLS LTD, and impaired rotarod performance. Additionally, Spino$^{\Delta dMSN}$ nor Spino$^{\Delta iMSN}$ impacted basal-, hyper-, or hypo-locomotion, suggesting these novel mouse lines are poised to identify cell type-specific mechanisms underlying repetitive and sequential motor programs.

## KEY RESOURCES TABLE

| Resource Type | Specific Reagent or Resource | Source or Reference | Identifiers | Additional Information |
|---|---|---|---|---|
| Add additional rows as needed for each resource type | Include species and sex when applicable. | Include name of manufacturer, company, repository, individual, or research lab. Include PMID or DOI for references; use “this paper” if new. | Include catalog numbers, stock numbers, database IDs or accession numbers, and/or RRIDs. RRIDs are highly encouraged; search for RRIDs at https://scicrunch.org/resources. | Include any additional information or notes if necessary. |
| Antibody | spinophilin-sheep | Thermo Fisher Scientific | RRID:AB_2605900 | |
| Antibody | SAPAP3-Rabbit | MilliporeSigma | ABN325 | |
| Antibody | mGluR5-mouse | MilliporeSigma | MABN540 | |
| Antibody | PP1g1-Goat | Santa Cruz | RRID:AB_2168091 | Discontinued antibody |
| Antibody | PP1a-Mouse | Santa Cruz | RRID:AB_628177 | |
| Antibody | D2R-mouse | Santa Cruz | RRID:AB_668816 | |
| Antibody | Homer1-mouse | Thermo Fisher Scientific | RRID:AB_2724465 | |
| Antibody | Flotillin1-mouse | Santa Cruz | RRID:AB_2106563 | |
| Chemical Compound or Drug | VU0360172-mGluR5 PAM | Tocris (Bio-technie). PMID: 20923853 | 4323/50 | |
| Deposited Data; Public Database | Proteomics database deposit | ProteomeXchange | PXD034053 and 10.6019/ PXD034053 | |
| Organism/Strain | Spinophilin floxed mouse line on C57Bl6/J strain | This paper | Spinofl/fl | |
| Organism/Strain | Spinophilin knockout (Ppp1r9btm1.1(KOMP)Vlcg/ Ppp1r9b) | Jackson Laboratories/ MMRRC | RRID:MGI:5759401 | |
| Organism/Strain | SAPAP3 Knockout | Jackson Laboratories | RRID:IMSR_JAX:008733 | |
| Organism/Strain | DRD1 Cre (B6.FVB(Cg)-Tg(Drd1-cre)FK150Gsat/Mmucd | MMRRC | RRID:MMRRC_036916-UCD | |
| Organism/Strain | A2A Cre (B6.FVB(Cg)-Tg(Adora2a-cre)KG139Gsat/Mmucd) | MMRRC | RRID:MMRRC_036158-UCD | |
| Organism/Strain | tdTomato (B6.Cg-Gt(ROSA)26Sortm14(CAG-tdTomato)Hze/J) | Jackson laboratories | RRID:IMSR_JAX:007914 | |
| Software; Algorithm | Proteome Discover™ 2.5 | Thermo Fisher Scientific | RRID: SCR_014477 | |
| Software; Algorithm | Prism | Graphpad | RRID:SCR_002798 | |
| Software; Algorithm | Ethovision | Noldus | RRID:SCR_000441 | |
| Tool | Phenotyper Cages | Noldus | RRID:SCR_004074 | RRID for Noldus Information Technology |
| Tool | LSM900 with AiryScan 2 | Zeiss | RRID:SCR_022263 | |
| Tool | Cytation 3 | Biotek/Agilent | Cytation3 | |